AFIT/GEP/ENP/91D-4

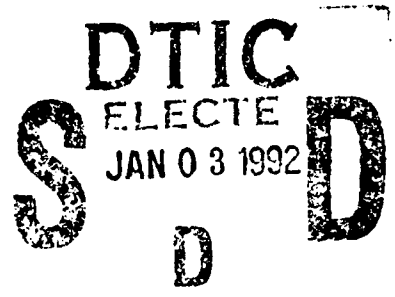

PHOTOLUMINESCENCE SPECTROSCOPY OF MBE GROWN GALLIUM ANTIMONIDE

THESIS

John A. Dorian, Captain, USAF

AFIT/GEP/ENP/91D-4

Approved for public release; distribution unlimited

AFIT/GEP/ENP/91D-4

PHOTOLUMINESCENCE SPECTROSCOPY OF MBE GROWN GALLIUM ANTIMONIDE

THESIS

Presented to the Faculty of the School of Engineering

of the Air Force Institute of Technology

Air University

in Partial Fulfillment of the

Requirements for the Degree of

Master of Science in Engineering Physics

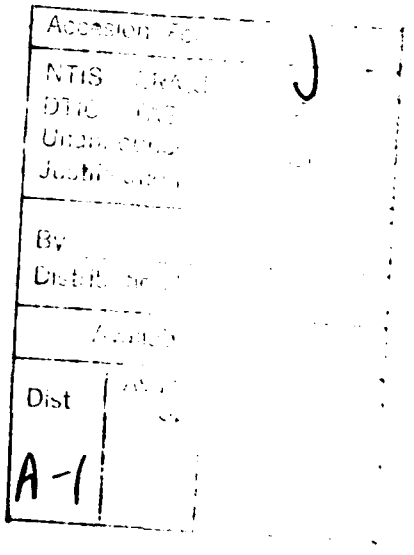

John A. Dorian, B.S.

Captain, USAF

December 1991

Approved for public release; distribution unlimited

December 1991 Master's Thesis

Photoluminescence Spectroscopy of MBE Grown Gallium Antimonide

John A. Dorian, Captain, USAF

Air Force Institute of Technology
WPAFB OH 45433-6583

AFIT/GEP/ENP/91D-4

Capt. Kevin J. Keefer
PL/LID
Kirtland AFB, NM 87117

Experimental data are presented for the energy levels of the native acceptor and bound exciton emissions of GaSb grown by MBE and studied with low temperature photoluminescence (PL) spectroscopy. The undoped GaSb emissions showed a donor-acceptor pair transition with an observed emission peak at 776 meV, a peak at 716 meV usually associated with the ionization level of the acceptor, and bound exciton transitions in the energy range from 796 to 804 meV. Other unidentified peaks were observed at about 805 meV. Temperature and power dependence studies of the acceptor peak confirmed donor-acceptor pair (DAP) behavior. A GaSb sample grown with a high antimony background pressure had emissions which were broad as compared to those emissions of a sample grown with a lower V:III flux. The full width at half maximum was 45 meV and was due to multiple peaks. A temperature dependence study aided in the identification of three separate emissions, assigned as follows: 772 meV, due to a DAP, and 760 and 751 meV due to a deep acceptor level associated with a free to bound transition. The broad emission of the undoped GaSb sample was compared with the emissions of a Te doped n-type GaSb sample.

Photoluminescence, Gallium Antimonides, Molecular Beam Epitaxy, Solid State Physics, Emission Spectra, Semiconductors, Group III Compounds 60

Unclassified Unclassified Unclassified UL

Acknowledgements

The fortitude and attitude to persist in my academic endeavors is the result of assistance from many quarters. I wish to thank Professors Robert L. Hengehold and Yung Kee Yeo for their guidance and tolerance of my progress in solid state research. The guidance of Captain Todd Steiner and Captain Jose Colon greatly assisted my efforts; I am indebted to you for your help and friendship. The opportunity to study the gallium antimonide samples was made possible by Captain Kevin Keefer of the Phillips Laboratory, in concert with Dr. Stephen Eglash of Lincoln Laboratory. I thank Mr. Greg Smith for his invaluable role of ensuring the CL system was either working or, through no fault of his own, nearly working.

My heartfelt appreciation and admiration go to my parents for their concern and encouragement. Most of all, my dearest Sandra has won my heart once again for her support, patience, and smile at the end of the day. I am grateful and I am blessed.

Johnny Dorian

Table of Contents

	Page
Acknowledgements	ii
List of Figures	iv
List of Tables	vi
Abstract	vii
I. Introduction	1
II. Theory and Background	3
Semiconductors	3
Luminescence	7
Previous Work	10
Molecular Beam Epitaxy	13
III. Experimental Procedure	15
Sample Preparation	15
Apparatus	16
Procedure	19
IV. Results and Discussion	21
N-Type GaSb	21
P^+ - N Junction	23
Undoped P-Type GaSb	24
V. Conclusion and Recommendations	39
Appendix 1	41
Appendix 2	42
Appendix 3	43
Appendix 4	44
Bibliography	50
Vita	52

List of Figures

Figure		Page
1.	Band Structure of Insulators, Conductors, and Semiconductors	4
2.	Exciton Energy Levels	5
3.	Crystal Structures of a) Diamond and b) Zincblende	6
4.	Radiative Transitions in Semiconductors	8
5.	Schematic of MBE Growth System	14
6.	Photoluminescence Experiment Laboratory	16
7.	Comparison Spectra for n-type GaSb with Different Substrates, GaAs (Sample 90-100) and GaSb (Sample 90-102)	23
8.	Spectrum of p^+-n GaSb Diode of Sample 90-081	24
9.	Comparison Spectra for Undoped GaSb Grown with Different Substrate Temperatures and Antimony Pressures for Samples 90-088, 90-097,and 90-098	25
10.	Two GaSb Spectra from Sample 90-250 at Two Different Positions	26
11.	Excitation Power Dependence Spectra of GaSb Sample 90-250	27
12.	Temperature Dependence Spectra of Intermediate Antimony Flux GaSb	29
13.	Temperature Dependence of Native Acceptor Peak Energy for Sample 90-088	30
14.	Temperature Dependence of Native Acceptor Peak Intensity for Sample 90-088	31
15.	Excitation Power Dependence Spectra of Intermediate Antimony Flux GaSb	32
16.	Excitation Power Dependence of Native Acceptor Peak Energy and Intensity for Sample 90-088	33
17.	Excitation Power Dependence Spectra of High Antimony Flux GaSb for Sample 90-097	34

Figure		Page
18.	Temperature Dependence Spectra of High Antimony Flux GaSb for Sample 90-097.....	35
19.	Cathodoluminescence Spectrum of Undoped GaSb.....	36
20.	Spectrum of $Al_{.5}Ga_{.5}As$:Er from Photoluminescence.....	38
21.	Spectra of $Al_{.5}Ga_{.5}As$:Er from Cathodoluminescence.....	38
22.	Cathodoluminescence Experiment Laboratory.....	45

List of Tables

Table		Page
1.	Properties of Gallium Antimonide.....	11
2.	Low Temperature Emission Features of Gallium Antimonide.....	12
3.	Growth Conditions of GaSb Samples 90-100 and 90-102 Grown on GaAs and GaSb Substrates, Respectively.....	22
4.	Growth Conditions of GaSb Samples 90-088, 90-097, and 90-098 Grown on GaSb Substrates.....	24
5.	Emissions from GaSb Sample 90-250 at 8 K.....	27
6.	Emissions from GaSb Sample 90-250 at 4 K.....	28
7.	Effect of Temperature on GaSb Sample 90-088.....	29
8.	Effect of Excitation Power on GaSb Sample 90-088.....	32
9.	Argon Laser Penetration into Gallium Antimonide at 300 K.....	41
10.	Laser Power Density.....	42
11.	Spectrometer Slit Adjustments.....	43

Abstract

Experimental data are presented for the energy levels of the native acceptor and bound exciton emissions of GaSb grown by MBE and studied with low temperature photoluminescence (PL) spectroscopy. The undoped GaSb emissions showed a donor-acceptor pair transition with an observed emission peak at 776 meV, a peak at 716 meV usually associated with the ionization level of the acceptor, and bound exciton transitions in the energy range from 796 to 804 meV. Other unidentified peaks were observed at about 805 meV. Temperature and power dependence studies of the acceptor peak confirmed donor-acceptor pair (DAP) behavior. A GaSb sample grown with a high antimony background pressure had emissions which were broad as compared to those emissions of a sample grown with a lower V:III flux. The full width at half maximum was 45 meV and was due to multiple peaks. A temperature dependence study aided in the identification of three separate emissions, assigned as follows: 772 meV, due to a DAP, and 760 and 751 meV due to a deep acceptor level associated with a free to bound transition. The broad emission of the undoped GaSb sample was compared with the emissions of a Te doped n-type GaSb sample.

PHOTOLUMINESCENCE SPECTROSCOPY OF MBE GROWN GALLIUM ANTIMONIDE

I. Introduction

Among the semiconductors fabricated of the Group III-V atoms, those fabricated from gallium arsenic indium antimonide (GaAsInSb), aluminum gallium arsenic antimonide (AlGaAsSb), and gallium antimonide (GaSb) have thus far been reported to be able to achieve a wide wavelength range of emissions, from 1.7 to 4.4 microns (μm) (1:669). There are some arrangements of these compounds which have been forged into devices which operate near 2.55 μm at room temperature. The creation of devices at this wavelength is significant for a number of potential applications including optical communications networks using fluoride based glass fibers with exceptionally low losses (2:5936) and laser radars exploiting atmospheric transmission windows within the range of 3 to 5 μm. The role of the GaSb substrate for these devices is crucial in achieving the desired operating wavelength.

The growth of GaSb by molecular beam epitaxy and characterization by photoluminescence have been sparsely studied. While the various growth conditions tend to produce similar but not identical spectra, doping levels can dramatically alter the spectra; there is slight information about the assignment of donor and acceptor energy levels to specific sources. In this research, the spectrum of GaSb was studied as a function of antimony flux, representing the Group V:III ratio, and

growth temperature as growth parameters. Parallels are drawn to the spectra of GaSb samples grown under different conditions. The information from this study can reveal data about the nature of the transition centers and the foundations of the electrical properties of GaSb.

As a technique, photoluminescence discloses the transition energies between various levels provided the transmission is radiative. The energy difference revealed must be less than the band gap of the material or else the energy will be reabsorbed, so the extent of the information is limited. An advantage of photoluminescence is its nondestructive nature. Other techniques can compliment photoluminesence results. The use of cathodoluminescence was attempted; however the success in observing GaSb emission was limited due to various detector and alignment issues. The cathodoluminescence spectra of an AlGaAs sample implanted with erbium was successfully obtained to calibrate system performance.

II. Theory and Background

Semiconductors

A semiconductor is a crystalline material which, at absolute zero, is a perfect insulator due to the inability of electrons to move and conduct charge. Yet, at increased temperatures, the semiconductor is able to conduct due to the presence of thermally excited electrons. The phenomenon of semiconductors is understood by the theory of allowed and forbidden energy bands, which is based on the quantum mechanic representation of solids.

The theory of solids infers the overlap of the electronic wave functions of the atoms and the subsequent formation of discrete energy bands for the electrons. The nature of the discreteness permits the electron to exist in some regions of energy and momentum, while in other regions the electron is forbidden. Electrons (fermions) will occupy the available bands starting at the lowest energy level and successively filling up higher levels.

Because it is the electrons which conduct current, those electrons in filled bands have no higher energy levels available to them and therefore do not conduct. If the energy gap between the topmost filled band and upper empty band is large, then the material is an insulator. On the other hand, if the electrons do not fill up the band and the material has many energy levels available for the electron to occupy, the material is a conductor. If the uppermost filled band is separated from a higher but empty band by a small energy spacing, the material is classified as a semiconductor, see Figure 1. The energy separation of

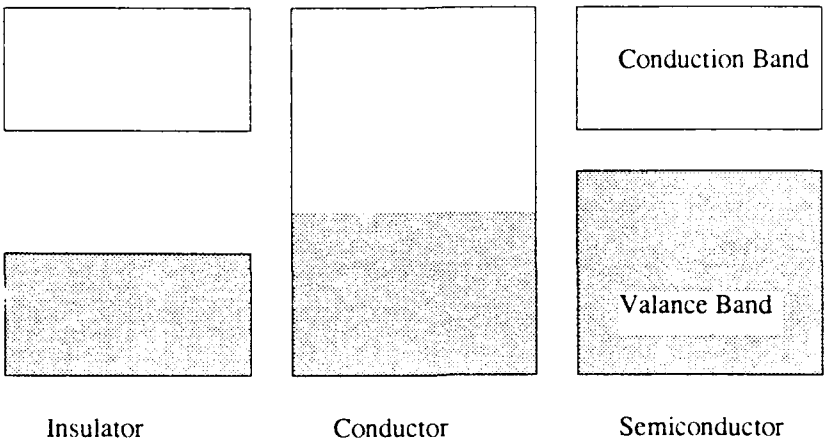

Figure 1. Band Structure of Insulators, Conductors, and Semiconductors

the highest filled band and the next empty or partially filled band is known as the energy gap, E_g.

When an electron is excited into a higher energy state, the vacant position left behind in the lower band acts as a positive charge. The excitation could be due to thermal effects, applied charge, or photoexcitation. The occurrence of the positive charge has been conceptualized as a hole, which is sufficiently identifiable and measurable to validate the unorthodox concept. An exciton is formed when a hole and electron experience an attraction due to Coulomb forces. An exciton is a mobile pair within the material which may overlap many atoms within the crystal (3:13). The ionization, or binding, energy for the exciton is given by (3:13):

$$E_{ex} = -m^* e^4 / 2h^2\epsilon^2 n^2 \qquad (1)$$

where

m^* is the reduced effective mass;

e is the electron charge;

ϵ is the dielectric constant of the material; and

n is a quantum number representing the exciton state

The reduced effective mass is given by:

$$1/m^* = 1/m_e + 1/m_h \qquad (2)$$

where

m_e is the electron effective mass; and

m_h is the hole effective mass

The exciton energy levels occupy positions just below the conduction band. Figure 2 represents the exciton energy levels and the possible recombinations.

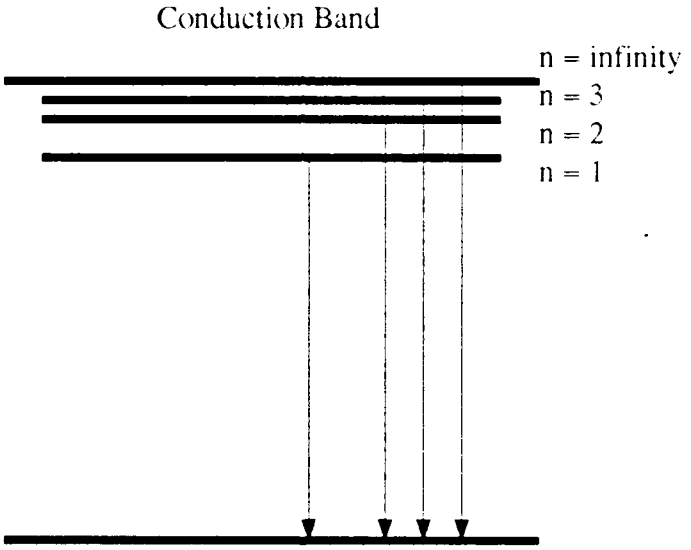

Figure 2. Exciton Energy Levels

For a semiconductor, the atoms in the material must exhibit a periodic symmetry in their structure. With such symmetry, the crystal can be assigned one of a number of lattice structures. GaSb forms a zincblende structure with four covalent bonds spaced as a tetrahedron about any atom. The zincblende structure is closely related to the

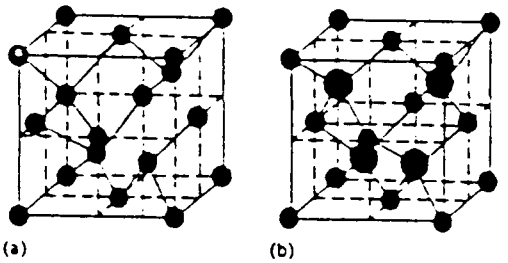

Figure 3. Crystal Structures of a) Diamond and b) Zincblende (4:15)

diamond lattice, both are based on the face centered cubic arrangement, as shown in Figure 3.

A change in the crystal structure from the perfect lattice is called a defect. Defects occur by a number of different means but one major defect is that of an impurity. The most modern production techniques still allow the development of impurities. The final result of such impurities is that energy levels develop within the band gap. The presence of energy levels within the band gap of the material indicates the impurity has resulted in the formation of electron or hole states within what is normally a forbidden zone.

Substitutional impurities can create additional energy levels known as donor or acceptor levels. The substitutional atom, while bonding with native atoms, may alter the coulomb electrostatic forces and shift the energy distribution. A donor energy level is located slightly below the bottom of the conduction band while acceptor levels are above the valence band. The donor occurs when the impurity has a valence greater than the atom it replaced, since the greater valence means it has electrons not needed for bonding; these electrons may be donated to other processes. GaSb is a semiconductor formed of periodic table Group III-V atoms. When an element from Group VI, such as

tellurium, is the impurity, it has an extra electron which is only loosely bound to the tellurium atom in the lattice. When the substitutional impurity is due to a Group II element, such as zinc, an acceptor level is formed due to the shortage of electrons. The shortage is filled in the process of creating a hole. The binding energy of the hole or electron to an impurity is similar to the exciton energy equation, however the interpretation of m^* is now the effective mass of the electron or hole (3:9). The electron or hole can be removed from the impurity if it is excited to the conduction or valence band; the impurity is now ionized with the loss of the charged particle.

Other defects in the crystal can also have significant effects on the semiconductor properties. The strain introduced by a lattice mismatch, for example a GaSb layer on a GaAs substrate, can alter the energy levels. A vacancy at a lattice point effectively creates an impurity, which can form either an acceptor or an acceptor complex, because the bonding needs are no longer being satisfied.

Luminescence

An electron can be induced to move from a lower to a higher energy level with a push from an external energy source. Once the material is in a non-equilibrium state, the electron may then seek to return to a lower energy state. The detection of the electron's radiative return is the basis for luminescence measurements. If the external energy source uses photons to excite the electrons the process named photo-luminescence, while if electrons are used to transfer the energy the process is cathodoluminescence. In each case, the emission of

photons during the radiative relaxation provides direct insight into the possible and probable transitions within the semiconductor.

The most common processes which result in luminescent peaks are band-to-band, free-to-bound acceptor, free exciton, free-to-bound donor, bound exciton, and donor-acceptor pair recombination, Figure 4. The transitions which have an energy greater than the band gap are not likely to be observed because the emissions are generally reabsorbed within the material.

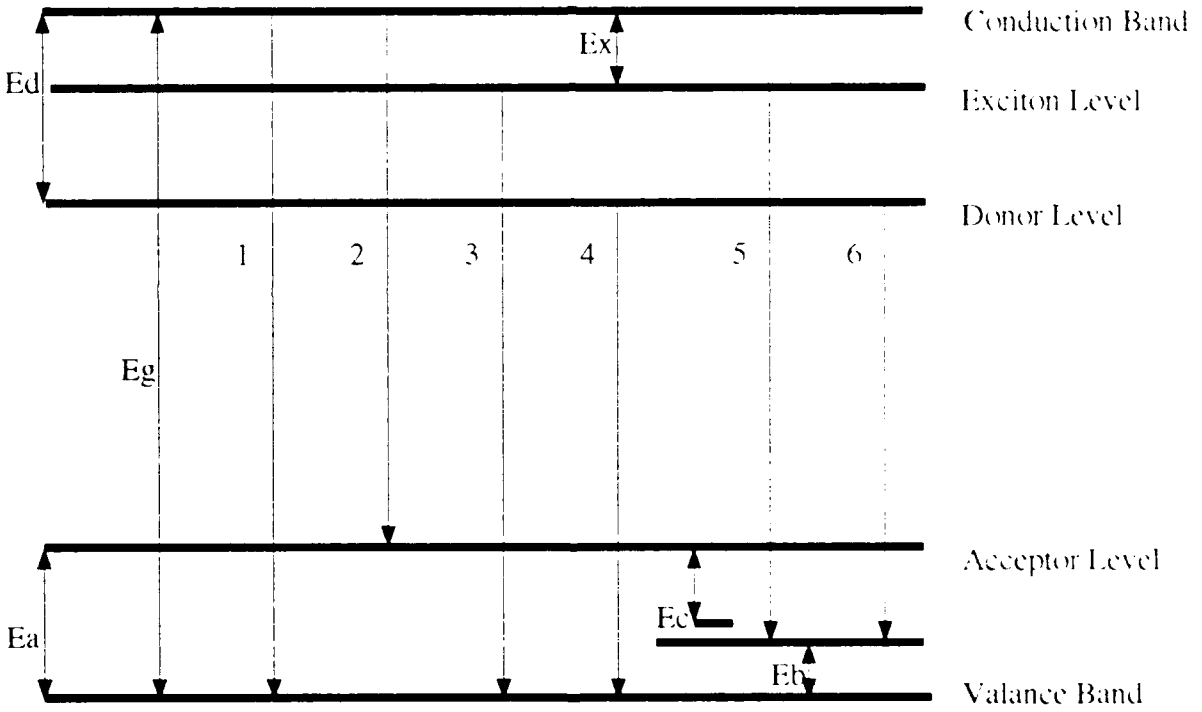

1. Band to Band
2. Free to Bound Acceptor
3. Free Exciton
4. Free to Bound Donor
5. Bound Exciton
6. Donor Acceptor Pair

Eg = Energy Gap
Ed = Donor Energy Level
Ea = Acceptor Energy Level
Ex = Exciton Binding Energy
Ec = DA Coulomb Binding Energy
Eb = Exciton Bound Energy

Figure 4. Radiative Transitions in Semiconductors

The transition of an electron directly from the conduction band to the valence band, resulting in recombination with a hole, is known as a band-to-band transition. The opposite transition is the key process in the excitation of electrons by photoluminescence or cathodoluminescence, referred to as the fundamental absorption (3:34). Band-to-band luminescence is not generally seen due to reabsorption and the need for high excitation levels to populate the other competing transitions.

The transitions between deep acceptor or deep donor levels and the band edge are strongly affected by the purity of the semiconductor (3:134). Large impurity concentrations, which reduce emission intensity, tend to form impurity bands, rather than an single energy level, and may merge with the intrinsic band of the material.

The donor-acceptor pair (DAP) transition involves an electron in a donor level combining with a hole at an acceptor level. The physical separation of the donor and acceptor sites is important since the DAP interact with a coulomb potential. The energy of the DAP transition is:

$$E = E_g - E_d - E_a + e^2/\epsilon r \qquad (3)$$

where e is the electron charge;

ϵ is the dielectric constant; and

r is the spacing between the donor and acceptor pair

The presence of exciton energy levels near the conduction band is another significant source of emissions. In pure materials the presence of unbound electrons and holes allows the free exciton to exist and recombine (3:114). The free exciton transition energy is:

$$E = E_g - E_{ex} \qquad (4)$$

When the exciton is bound to an impurity the binding energy is characteristic of the impurity and alters the transition energy to:

$$E = E_g - E_{ex} - E_b \quad (5)$$

In both of these cases the $1/n^2$ factor results in a series of excited states and emission peaks, but competing processes and the low intensity of the emissions can obstruct their observation.

Since GaSb is a direct band gap material no phonons are necessary to conserve momentum during the recombination of an electron and a hole. However, the dynamics of the crystal lattice readily insures the involvement of optical phonons in the emission process. The transfer of energy by phonons proceeds with longitudinal optical (LO) phonons being most preferred since it exhibits the strongest change in potential energy per unit of displacement (3:113).

Previous Work

The semiconductor gallium antimonide has been studied for over thirty years. Characterization efforts prior to 1985 concentrated on the results of liquid phase epitaxy (5:177), vapor phase epitaxy, metalorganic vapor phase epitaxy, and solution grown bulk crystals (6:2382). A good summary is provided by Lee (7:2895). Since 1985, molecular beam epitaxial grown crystals of gallium antimonide have merited considerable attention.

GaSb is a direct gap semiconductor with the properties listed in Table 1. One aspect of the crystal which differentiates it from some Group III-V semiconductors, but is similar to gallium arsenide, is the presence of a subsidiary conduction minima in the [111] crystal direction about 50 to 100 milli-electron volts (meV) above the band gap (10:147, 11:361). The transitions observed in photoluminescence from GaSb are listed in Table 2. It is a p-type material when created by the

Table 1. Properties of Gallium Antimonide (8:1005, 9:16)

Property	Value	Units
molecular weight	191.48	g
density	5.613	g/cm^3
crystal type	Zinc Blende	
lattice parameter	6.094	Å
refractive index (1.3-2.5μm)	3.8	
dielectric constant	15.69	
mobility		
electron	4000-5000	$cm^2/V*sec$
hole	850-1400	
Effective mass		
electron	0.042	m^*/m_0
hole	0.40	
bandgap		
300 K	722	meV
0 K	812	meV

most common growth techniques. Current reports strongly concur in identifying the native acceptor in GaSb as an intrinsic complex formed by a gallium vacancy and a gallium antisite defect (V_{Ga},Ga_{Sb}). The complex is known to be a double acceptor, with ionization levels at 33 and 80 meV above the valence band (13:1093), with the literature suggesting a range of values.

The band gap of GaSb is known to be 812 meV at 0 Kelvin (K). The temperature dependence of the band gap is given by (14:352):

$$E_g(T) = 0.812 - 0.00042 * T^2/(T + 140) \quad (6)$$

With this knowledge of the band gap, the free exciton energy level can be calculated using the analogy of the hydrogen atom representing the orbiting electron and the hole. The binding energy of the exciton is 2.08 meV, from Equation (1) with n = 1; therefore the free exciton transition energy is 810 meV.

The effect of intentional impurities in GaSb has been studied with both electrical and photoluminescence methods for the following dopants: germanium (15:1215), zinc (16:1427), silicon (17:1030), tellurium (14:350, 17:1030, 18:1645), and sulfur and selenium (18:1645). The luminescence of GaSb is very strongly affected by dopant concentration, as noted in n-type tellurium doped GaSb by Baranov (17:1030).

Table 2. Low Temperature Emission Features of Gallium Antimonide

Transition	Notation		Energy (meV)	Wavelength (Å)	Ref.
free exciton	FE	(X)	810	15306.7	8
unidentified	U		807.95 -808.7	15345.5 -15331.3	8
exciton bound to neutral acceptor	BE1	(A°,X)	805.4	15394.1	6
	BE2		803.4	15432.4	6
	BE3		800.1	15496.1	6
	BE4		796.1	15574.0	6
unidentified			795	15595.5	8
conduction band or donor-acceptor	P	(e,A°) (D°,A°)	783.8	15824.4	8
native acceptor	A	(D°,V_{Ga}-Ga_{Sb})	777.5	15946.5	6
phonon replica	BE4-LO		765	16207.1	6
donor acceptor	B	(D°,A°)	758	16356.8	6
phonon replica	A-LO		748.5	16564.4	6
phonon replica	B-LO		728	17030.8	6
second ionization level of native acceptor	A^-	(D°,V_{Ga}-Ga_{Sb}^-)	710	17462.7	6
LO phonon			28		12
TO phonon			27.3		12

The nature of the GaSb material is crucial when the GaSb is the substrate for other semiconductors. As antimony based tertiary and quaternary semiconductors are grown, the characteristics of the substrate plays a vital role. The use of GaSb and GaInSb to form quantum well structures was reported by Haywood (19:922), and the investigation of GaAsInSb films was reported by Bochkarev (15:1215). A band gap variation of 25 meV, due to lattice matching of GaAsInSb onto (100) and (111) GaSb when grown by liquid phase epitaxy, has been reported (2:5936). For molecular beam epitaxial growth of GaAsInSb/AlGaAsSb on Gasb, the lattice matching was also found to be crucial; slight variation in the composition of the GaAsInSb and AlGaAsSb significantly altered the energy gap. These quaternary alloys have recently shown promise as a room temperature diode laser emitting near 2.3 μm (20:207).

Molecular Beam Epitaxy

Growth of semiconductors by molecular beam epitaxy is relatively recent, yet the high quality products possible with this technique have already pushed the method into the commercial production of MBE chambers. The advantages of MBE growth are: 1) a slow growth rate allows composition changes on the atomic scale, 2) low growth temperature minimizes interdiffusion, 3) sequential deposition of the materials required for buffer and ohmic contact regions is possible, 4) physical masks can be inserted or withdrawn to aid in creating the desired three dimensional structure, and 5) the vacuum environment permits the monitoring of chemical and structural properties, throughout the growth duration, by a variety of surface probing techniques (21:17).

An MBE system consists of beam generators, beam interrupters, substrate holders, growth monitors, and the enclosing chamber, as shown in Figure 5. One or more beam generators are the source of high purity atomic or molecular beams. The generators face the substrate but are subject to blockage by the interrupters, which are mechanical shutters

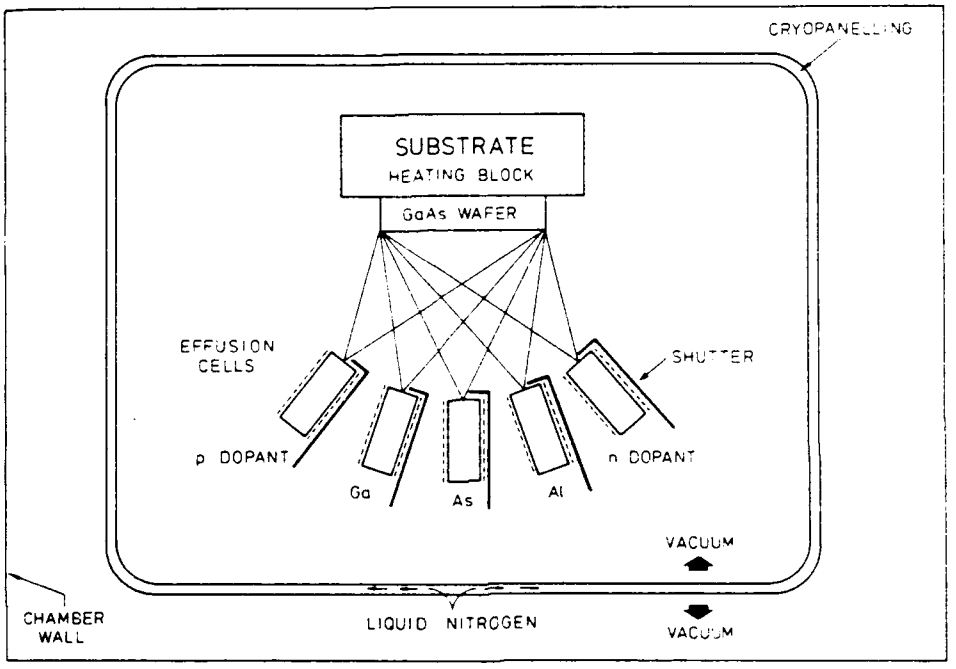

Figure 5. Schematic of MBE Growth System (21:17)

to block the direct path from the source to the substrate holder. The holder provides the uniform and reproducible temperatures needed to assure a high quality surface. Monitors, such as mass spectrometers, ionization gauges, and reflection high energy electron diffraction devices, are vital to proper characterization of the growth environment. The vacuum chamber, capable of pressures of less than 10^{-10} torr, is constructed of selected materials and includes a liquid nitrogen cryopanel to aid in the removal of background contaminants (21:20).

III. Experimental Procedure

The GaSb and GaAsInSb samples used in the experiment were grown prior to the experiment by Dr. Stephen Eglash and his technical staff at the Massachusetts Institute of Technology's Lincoln Laboratory, Lexington, Massachusetts. The samples were handled carefully and cleaned thoroughly before and during the experiment. The equipment used to measure the luminescence of the samples included vacuum, cryogenics, laser, electron gun, and data recording devices.

Sample Preparation

The GaSb samples were stored, cleaned and mounted for examination in accordance with the standard practices of the Department of Engineering Physics. Samples were received in Fluoroware containers and kept in either protective envelopes or the original container. The dimensions of the samples were usually 3 millimeter (mm) by 6 mm. Prior to the first data recording, and later as required, the samples were cleaned. The cleaning accomplished the removal of any surface dust or grease film which might degrade the results. The cleaning process consisted of wetting, in sequence, with trichloroethylene, acetone, and methanol. During each spraying, care was taken to not permit the liquid to evaporate and leave a film. While still damp with methanol, the sample was blown dry with either dichlorodifluoromethane or dry nitrogen gas. The mounting of each sample on the apparatus cold-finger was done using cleaned tweezers. The samples were held in place with rubber cement, providing good thermal contact as well as adequate adhesion at

all temperatures. The rubber cement was spread in a band across the back of the sample, covering 25 to 50 percent of the back surface.

Apparatus

The luminescence of the samples was measured in a chamber in which cold gaseous or liquid helium would cool the sample. The sample was cooled using a liquid helium dewar and regulated with a temperature controller which employs resistive heaters. The excitation mechanism was predominantly with a laser, although an electron gun was used for comparison in a separate chamber, as described in Appendix 4. The luminescent signal was collected with lenses into a spectrometer and detector. The signal from the detector was amplified and then recorded and stored on a computer diskette. See Figure 6.

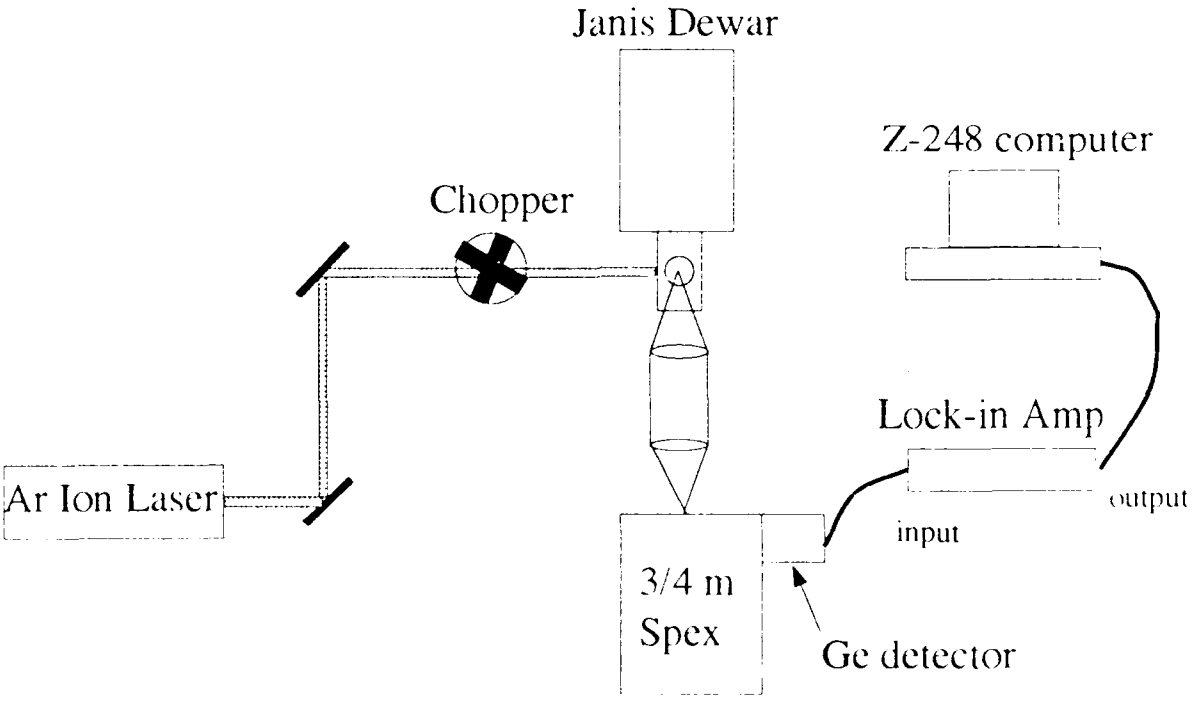

Figure 6. Photoluminescence Experiment Laboratory

A Janis Research Detachable Tail Research Dewar, Model 10DT, metered liquid helium from the storage dewar to the sample chamber. The walls of the dewar were kept in an evacuated condition by a Leybold-Heraeus turbomolecular pump, a Turbovac TMP-360. The samples were mounted on a copper finger attached to a specimen holder. The finger could hold up to eight samples at one time, and the holder could be rotated and raised or lowered to allow optimum positioning of any sample. Also on the finger were resistive heaters and temperature sensors. A Lake Shore Cryotronics temperature controller, Model 805, measured the temperature and operated the resistive heaters. The temperature controller applied current to the heaters when it sensed a difference between a preset and the measured temperature. Temperature control was accurate to 0.02 K, with a lower temperature bound of 2.0 K achieved during the experiment. For a 1 K temperature the sample was immersed in liquid helium and a mechanical roughing pump used to lower the vapor pressure of the helium below the lambda point.

The primary excitation mechanism for this experiment was 488 nanometer (nm) laser radiation. A Spectra-Physics Argon Ion laser, Model 171-17 with a power supply, water conditioner, and laminar flow unit was available to perform these photoluminescence experiments. The laser beam power ranges from 1 to 18 Watts, however an Oriel band pass filter used with the experiment limited the effective laser power to 2 to 220 milliwatts (mW) in most cases. Information about the photon penetration into GaSb is in Appendix 1. The beam power was measured with a Coherent Power Meter, Model 210. The laser beam was interrupted with a Scitec Instruments optical chopper linked to a lock-in amplifier.

The emissions from the excited sample were collected and detected to create a signal which could be accurately and rapidly recorded. The emission, after passing through the cold chamber window, was collected and focused by a lens system. Two glass lenses were used to collect and focus the emission through a 1 μm long-pass filter onto the entrance slit of the spectrometer.

A Spex 3/4-meter Czerny-Turner 1702 Spectrometer was used to separate the emitted luminescence into different wavelengths. The scan rate was typically 100 Angstroms per minute. The grating used in conjunction with the detector was a 600 lines per millimeter, 1.2 μm blazed grating.

An Applied Detector Corporation germanium detector, Model 403L, was used to obtain data on the GaSb samples. This detector covered a range from 800 nm to 1800 nm. It was kept at liquid nitrogen temperatures during operation and a bias voltage of -200 Volts was provided by a North Coast Scientific Bias Supply, Model 823A. The muon filter, Model 829B, was used on the recommendation of the manufacturer. The signal from the germanium detector was fed into the amplifier, as described below. The sensitivity of the germanium detector decreases at the upper wavelength limit, but it proved satisfactory.

The detector was connected to a Scitec Instruments 500MC Lock-In Amplifier. The two inputs to the amplifier were the reference signal from the chopper and the detector signal. The device amplified only the luminescence signal, excluding the background signal, by comparing the frequency of the chopper and the signal. Any background signal would not possess the same reference frequency since it was not interrupted by the chopper. Typical settings for GaSb measurements were a time

constant of 300 milliseconds and a sensitivity of 30 millivolts. The output of the amplifier was sent to a MetraByte STA-16 DAS-16 Accessory board which was matched to a MetraByte DASH-16 internal data acquisition board in a Zenith Data Systems Z-248 computer. The software used to monitor the data collection was Labtech Notebook. Typically, data was collected at a rate of six Hertz for a duration of ten minutes. The data was recorded on diskette in ASCII format and was available for manipulation and plotting by many routines, including the spreadsheet Quattro Pro.

Procedure

The cooling for the sample was accomplished by allowing the liquid helium to transfer from the vacuum enclosed dewar into the low pressure chamber. The helium pooled beneath the sample and subsequently chilled it. A crude temperature control was available from the transfer valve, while the temperature controller raised and effectively maintained the temperature at the selected set point.

The initial preparation of a data run included steps involving the spectrometer, the laser, and the optics. The range and scan rate required for the spectra scans were determined after the first scans, which covered a wide spectral range. Based on the intensity of the signal the minimum slit width was chosen. The laser power was measured before the spectral data was recorded, and the laser beam positioned with the periscope mirrors for the best signal. The interference filter and lenses were also adjusted on a sample by sample basis to improve signal intensity. It was a cyclic process. Oriel spectral lamps of argon were used to assure the calibration and resolution of the

spectrometer and detector set-up at the start of the experiment. For the weakest signals, the resolution of the experiment was about 35 Å, the equivalent of about 1.7 meV at 1.58 μm. The resolution was much better for more intense luminescence. The start of the spectral scan was done with a manual start of the data recording computer when the desired wavelength was passing through the spectrometer dial. The inherent possibility of a mistimed data recording leads to an uncertainty of 1.2 meV in the results.

In the analysis of data, a number of factors warrant being mentioned. The data was recorded as a function of time, which could be specifically matched to a wavelength interval. The wavelength data was converted to energy with a factor of 12398.42 electron volts-Angstrom. The intensity measurements do not account for system response, such as detector responsivity, grating linearity, or atmospheric absorption. The volume of data collected in each scan required averaging the data points prior to plotting and analysis. The number of points averaged was based on the data rate, noise in the signal, and the requirement of a final data quantity of 600 to 800 data point per scan. The use of the averaging program further removed some of the resolution in the data.

IV. Results and Discussion

Seven samples of GaSb were examined by spectroscopic photoluminescence. The growth and doping conditions of the samples varied and provided the basis for the investigation. The luminescent emissions were anticipated to occur in the energy region from 700 to 815 meV, or in wavelength from about 15200 to 17750 Angstroms (Å).

The spectra of the seven samples provided a mixture of emissions that could be associated with the growth conditions of the sample. Some exhibited emissions that are typical of undoped p-type GaSb, while in others the emission spectra were significantly altered. In an attempt to better resolve emissions, the sample with the most intense emission was observed at a few settings of incident power. With greater detail, the temperature and incident power dependence of two samples was measured to aid in the analysis.

In order to obtain a greater understanding of the luminescence of GaSb and GaAsInSb, the cathodoluminescence emissions were included in the experiment planning. Unfortunately the spectra of the GaSb samples were observed with limited success due to difficulties with the experimental set-up. With the intention of validating system performance, the cathodoluminescence equipment was used to observe emissions in the region of 15400 Å from a sample of AlGaAs implanted with the rare earth element erbium. A comparison of photoluminescence and cathodoluminescence spectra provided encouraging results on the potential for further cathodoluminescence experiments.

N-type GaSb

The spectra from two samples provided the opportunity to observe the effects of doping GaSb with tellurium (Te) as well as the effects of a lattice mismatch between the GaSb epitaxial layer and a GaAs subordinate layer. Sample temperature was 8 K and the laser output was 100 mW. See Table 3 for a summary of the growth conditions.

Table 3. Growth Conditions of GaSb Samples 90-100 and 90-102 Grown on GaAs and GaSb Substrates, Respectively

Sample	Surface Layer Depth (μm)	Dopant	Dopant Temp. (°C)	Antimony Pressure ($x10^{-6}$ torr)	Substrate	Substrate Temp. (°C)
90-100	2.25	GaTe	475	1.64	GaAs	530
90-102	0.75	GaTe	475	1.38	GaSb	530

Electrical Van der Pauw measurements of sample 90-100 at 77 K place $n = 1.2 \times 10^{18}$ cm^{-3} and $\mu = 3260$ $cm_2V^{-1}sec^{-1}$ (22). The spectra for these samples is in Figure 7. The lattice mismatch effect is evident in the decrease in intensity of the emission from sample 90-100. Lee observed a decrease in the intensity of the 770 meV peak for lattice mismatched MBE grown GaSb (7:2899), the 770 meV emission is most likely related to the native acceptor and the tellurium donor level. The emission from each sample was maximized with care during the experiment and therefore the difference is not due to excitation or detection alignment variation. The doping with tellurium creates n-type GaSb. This choice of donor has been shown to radically change the luminescence spectra; the change correlates to the electron density changes (17:1031). The peak at about 755 meV gives credence to the existence of a Te-related

deep acceptor complex at an energy level 55 meV above the valence band. The deep level associated with Te by Poole (18:1646) could not be observed with this experimental set-up.

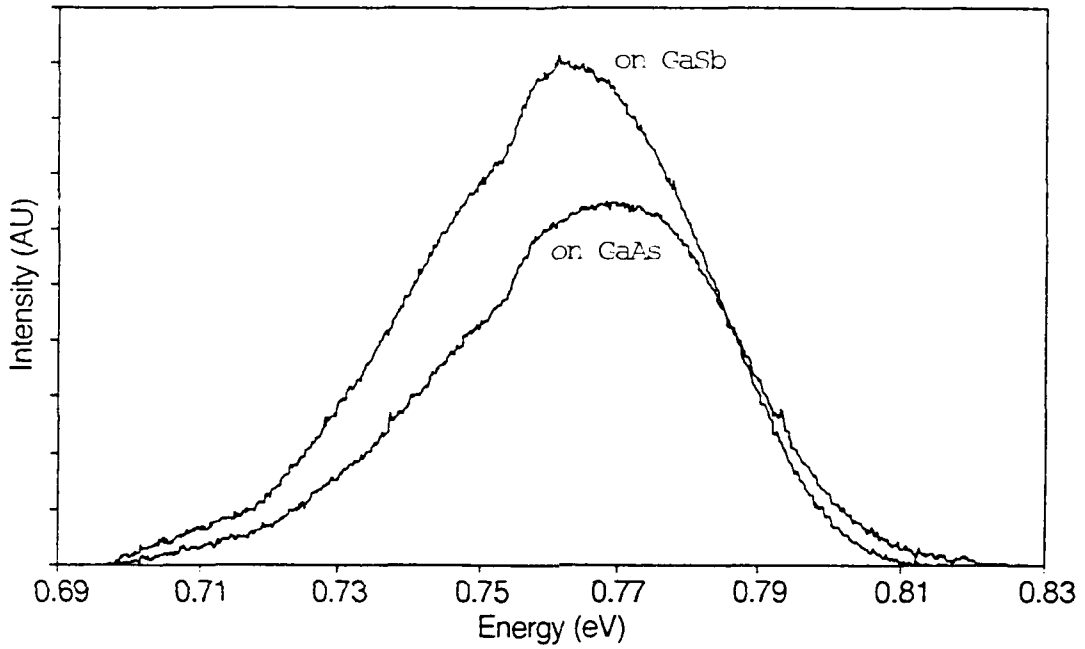

Figure 7. Comparison Spectra for n-type GaSb with Different Substrates, GaAs (Sample 90-100) and GaSb (Sample 90-102)

P^+ - N Junction

A spectrum of sample 90-081, Figure 8, was measured to observe the p-type GaSb associated with the p^+-n diode structure. Sample temperature was 8 K and the laser output was 100 mW. For this sample the 0.5 μm p-type GaSb top layer (N_A = 5 x 10^{18} cm^{-3}) is above a 2.0 μm n-type GaSb layer (N_D = 10^{16}-10^{17} cm^{-3}) on an n-type GaSb substrate. This sample was not examined further during the course of the research, therefore no speculation on the origins of the emission peaks at 807, 785, and 737 meV is warranted.

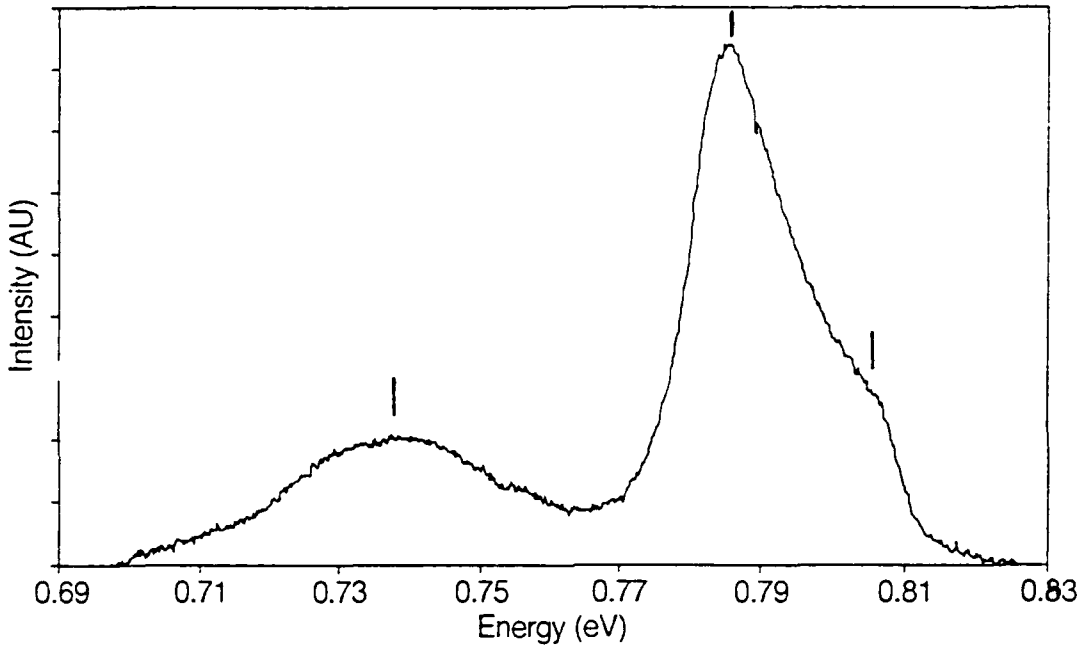

Figure 8. Spectrum of p^+-n GaSb Diode of Sample 90-081

Undoped P-type GaSb

Three samples were considered to be a set for the purpose of growth characterization of GaSb. The variation of antimony flux and substrate temperature for the undoped GaSb samples is summarized in Table 4. The luminescence of traditionally grown GaSb was observed in

Table 4. Growth Conditions of GaSb Samples 90-088, 90-097, 90-098 Grown on GaSb Substrates

	Surface Layer Depth (μm)	Antimony Pressure ($x10^{-6}$ torr)	Substrate Temperature (°C)
90-088	1.0	1.90	530
90-097	1.0	2.46	530
90-098	1.0	1.62	550

sample 90-088, while a broad luminescence, with a full width at half maximum (FWHM) of 42 meV, was observed in sample 90-097, as shown in Figure 9. A discussion of the emission peaks will be postponed until later in this document. Sample temperature was 8 K and the laser output was 100 mW. Due to the strong intensity of the emission from these two samples, they were selected for further study, which is described below. Further examination of sample 90-098 included only a brief examination of a temporal effect of the laser excitation and excluded investigation into the origin of the emissions at 807 and 740 meV.

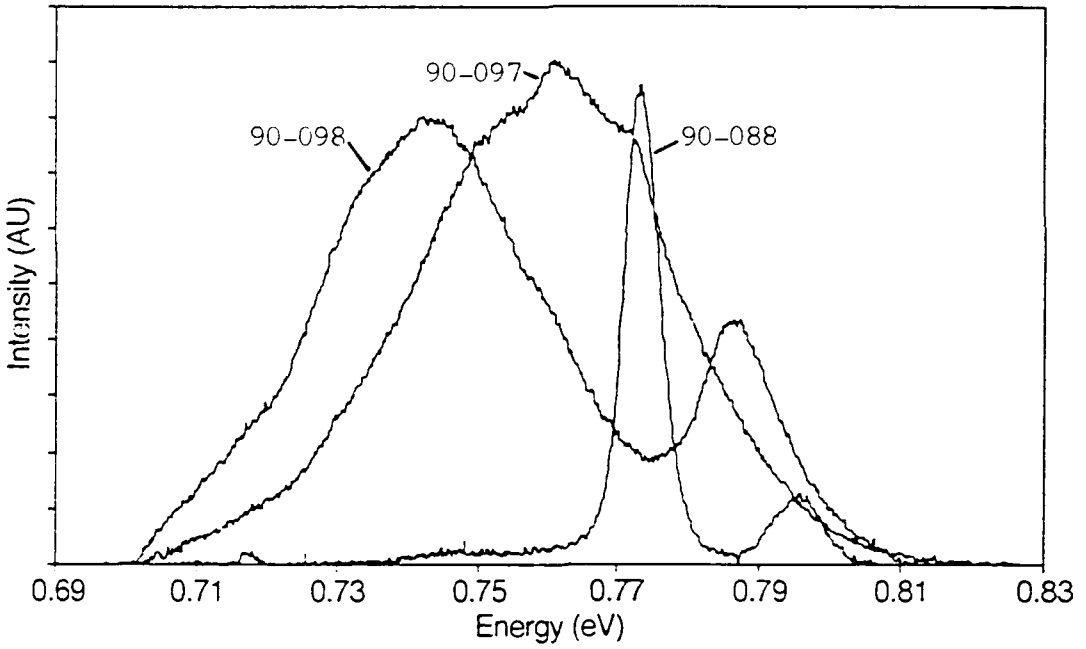

Figure 9. Comparison Spectra for Undoped GaSb Grown with Different Substrate Temperatures and Antimony Pressures for Samples 90-088, 90-097, and 90-098

Sample 90-250 was noted to exhibit the luminescence features associated with GaSb grown by techniques other than MBE. The initial excitation of the sample, Figure 10, was done in two positions on the

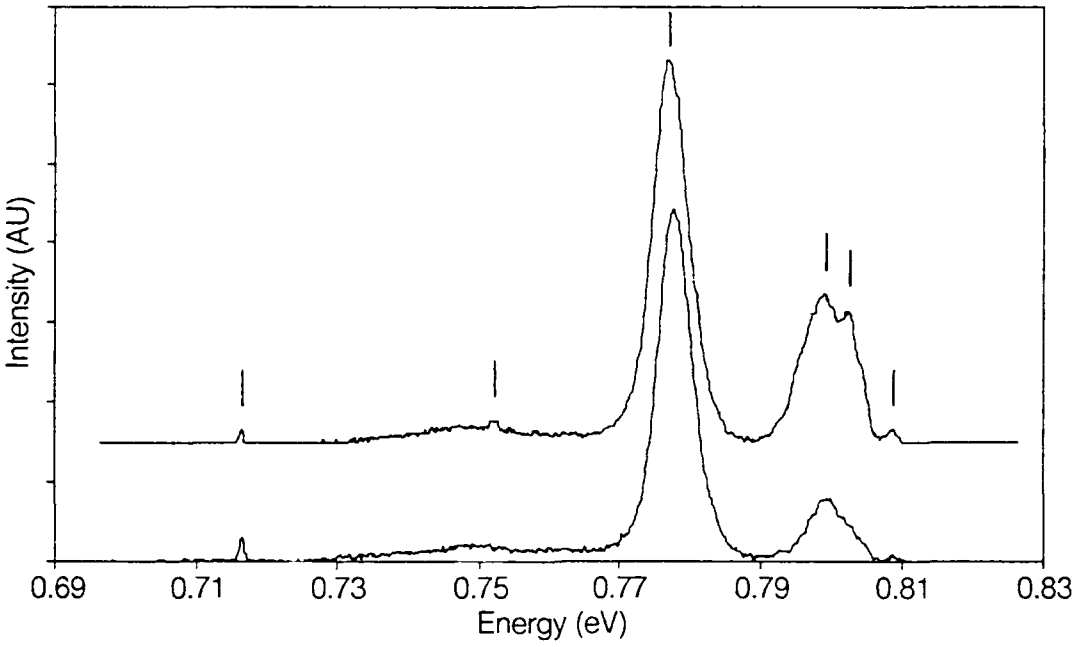

Figure 10. Two GaSb Spectra from Sample 90-250 at Two Different Positions

same sample. Sample temperature was 8 K and the laser output was 100 mW. The difference in intensity of the bound exciton emissions, especially at 802 meV, and the slight shift of the A transition, from 777.4 meV (lower) to 776.8 mev (upper) are indicators of possible inhomogeneity of this sample. The inhomogeneity was later observed in other samples, notably 90-098 and 90-097. This sample consisted of 2 μm GaSb on an n-type GaSb substrate. During growth the substrate temperature was 530 °C, the antimony pressure was 1.93×10^{-6} torr, and the arsenic temperature was 125 °C, leading to an arsenic pressure of about 10^{-9} torr. In these two spectra, the identifiable emissions are listed in Table 5.

Sample 90-250 was briefly investigated in the high energy portion of this spectra with the sample temperature at 4 K. In Figure 11, the emissions are shown for laser powers of 20, 40, and 70 mW. Even with

Table 5. Emissions from GaSb Sample 90-250 at 8 K

Source (see Table 2)	Energy (meV, ±0.28)
Unidentified	808.7
BE2	802
BE3	798.8
A	776.8 (upper), 777.4 (lower)
A-LO	749.4
A^-	716.4

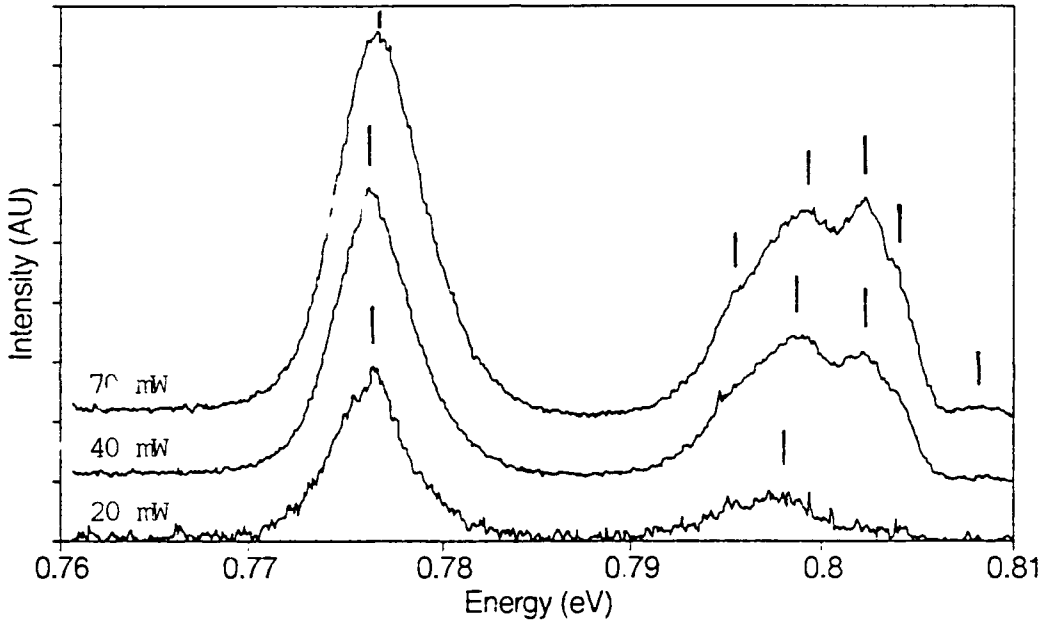

Figure 11. Excitation Power Dependence Spectra of GaSb Sample 90-250

these low powers, a general trend of the 776 meV emission envelope to higher energies is noted; observe the larger spacing between the three curves on the high energy side of the peak. This is indicative of the donor-acceptor-pair transition associated with the native V_{Ga}-Ga_{Sb} acceptor complex (13:1093). The emissions noted above 795 meV are associated with bound excitons (BE) (7:2896). The energies of the peaks are listed in Table 6. The increase in the intensity of the BE

transitions as the excitation power increases is expected up to the level where the recombinations via that emission balance the availability of free carriers (23:111). That level is not attained when the laser is operating at 70 mW. The intensity of the excitonic features may actually increase to levels higher than the native acceptor, depending upon growth conditions (24:299, 7:2898).

Table 6. Emissions from GaSb Sample 90-250 at 4 K

Source (see Table 2)	Energy (meV, ±0.36)		
	at 20 mW	at 40 mW	at 70 mW
Unidentified			808
BE1			804.0
BE2		802.2	802.3
BE3	798.0	798.5	799.2
BE4			795.3
A	776.2	776.2	776.7

The dependence of the emission on temperature and excitation power is a revealing investigation. The origin of peaks can be surmised with surprisingly few spectral scans. Both samples investigated for temperature and power dependence were grown at a substrate temperature of 530 °C; for the antimony pressure during growth, sample 90-088 was 1.90×10^{-6} torr, and sample 90-097 was higher at 2.46×10^{-6} torr.

The temperature region explored for sample 90-088 was 2 to 45 K. The 773 meV transition disappeared above 45 K and, though other transitions might have appeared, the study was halted. In Figure 12 is the spectra from six of nine different temperatures. In Table 7 are the GaSb band gap energy, the energy of the peaks, the FWHM, and the integrated intensity as temperature changes. The integrated intensity

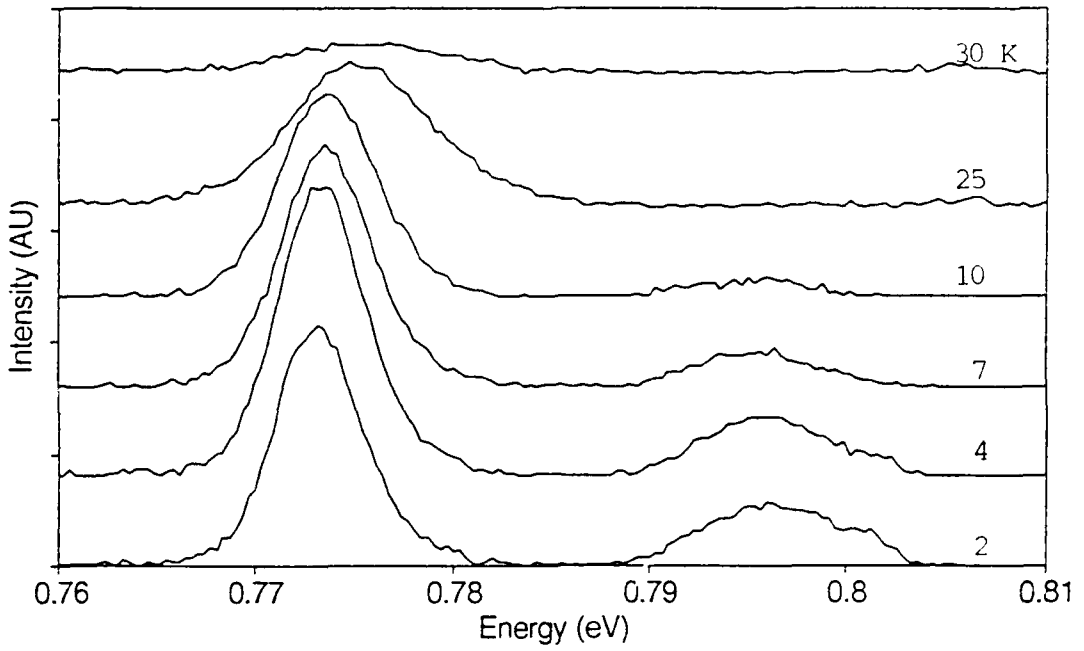

Figure 12. Temperature Dependence Spectra of Intermediate Antimony Flux GaSb

Table 7. Effect of Temperature on GaSb Sample 90-088

Temperature (K)	Bandgap (meV)	Peak Energy (meV)	FWHM (meV)	Intensity (arb. units)
2	811.99	773.2	5.2	55.6
4	811.95	773.4	5.2	67.3
7	811.86	773.5	5.1	55.3
10	811.72	773.6	5.6	51.1
15	811.39	774.1	6.8	42.2
20	810.95	774.5	7.4	41.9
25	810.41	774.8	8.4	18.5
30	809.78	775.6	10.4	4.7

was calculated by multiplying the height of the peak and the FWHM. Due to the averaging of the data the error in the peak position and the FWHM is ±0.3 meV. The shift of the peak and the shift relative to the band gap energy are shown in Figure 13. The shift to higher energies can be explained as follows. At very low temperatures, the electron will

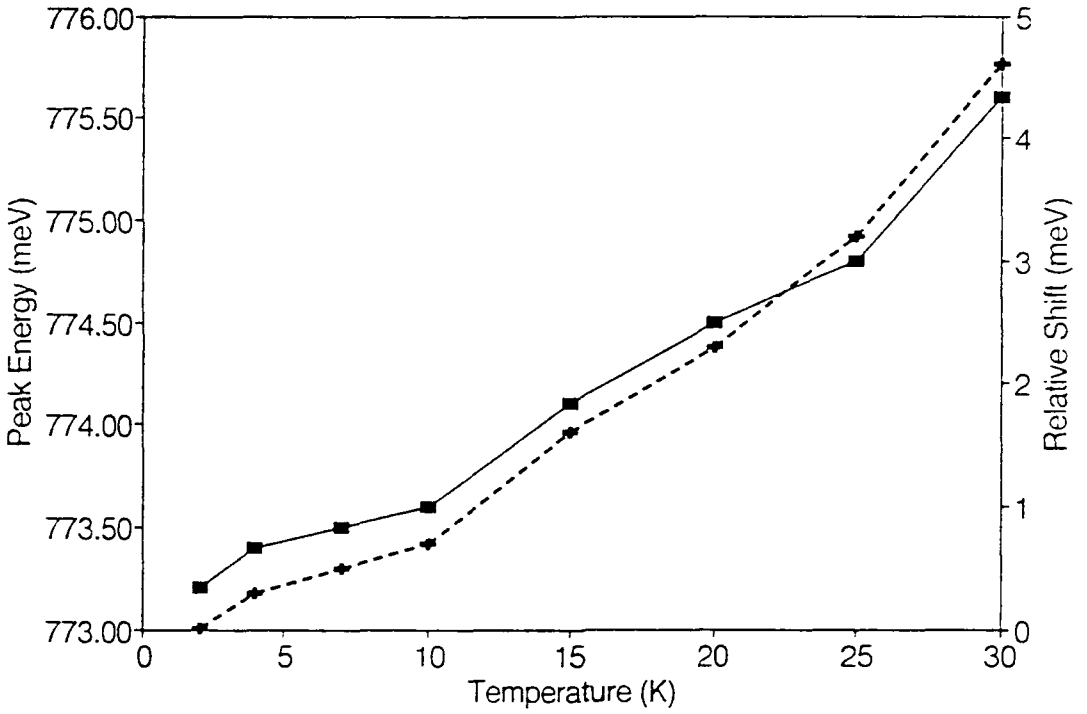

Figure 13. Temperature Dependence of Native Acceptor Peak Energy (solid) and Shift Relative to Band Gap (dash) for Sample 90-088

recombine from the donor level where it is strongly bound and thus donor-acceptor pair transitions prevail. However, donors become ionized as temperature rises and so the dominant transition is now a free-to-bound acceptor type. The binding energy of the donor could be approximately represented by the value of the shift if the intensity had not gone to zero at elevated temperatures. The integrated intensity of the 773 meV peak is plotted versus temperature in Figure 14. As the temperature increases, the emission intensity decreases because of the ionization of the donor, and also may be partly due to native acceptor. Nicholas has tracked the intensity of the 775 meV first ionization level and the 710 meV second ionization level, and noted the intensity of the second level continues to increase above 15 K, until it too starts to be ionized as the Fermi level crosses it above 50 to 60 K (24:301). The

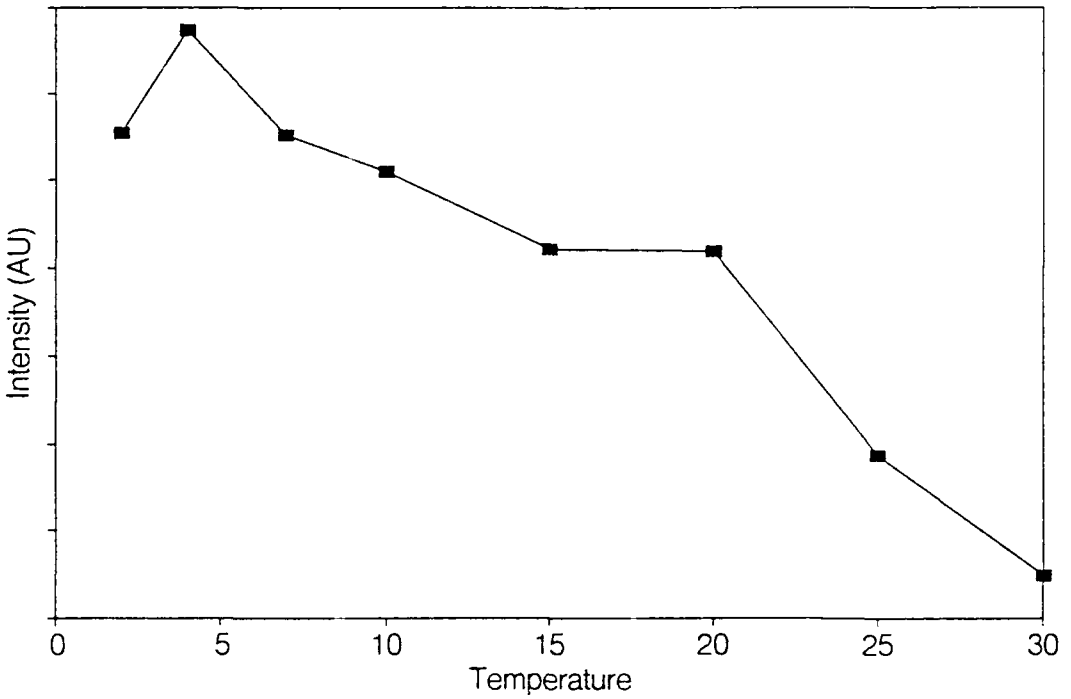

Figure 14. Temperature Dependence of Native Acceptor Peak Intensity for Sample 90-088

disappearance of the 796 meV emission is consistent with the temperature effect on the dissociation of acceptor bound excitons. The 805 meV emission that is starting to become apparent at 30 K is more pronounced at 45 K and may be due to the an ionized acceptor related transition at those elevated temperatures.

The laser power was varied between nine settings over the range of 2 to 500 mW at a temperature of 4 K, and the luminescence was recorded. In Table 8 are the data on peak position and intensity. The peak energy and FWHM estimation error is ±0.1 meV. The shift of the peak with power is due to the saturation of long distance donor-acceptor pairs. The portion of the intensity due to the distant pairs is fixed, but the nearer donor-acceptor pairs have a shorter recombination lifetime as well as emission at a higher energy. The expected narrowing of the

Table 8. Effect of Excitation Power on GaSb Sample 90-088

Power (mW)	Peak Energy (meV)	FWHM (meV)	Intensity (arb. units)
2	772.3	5.0	2.2
20	773.0	4.8	15.1
40	773.2	5.3	29.0
50	773.2	5.1	31.6
100	773.3	6.0	37.8
140	773.5	5.8	40.4
200	773.5	5.5	44.1
220	773.7	6.2	49.8
500	775.2	8.6	90.3

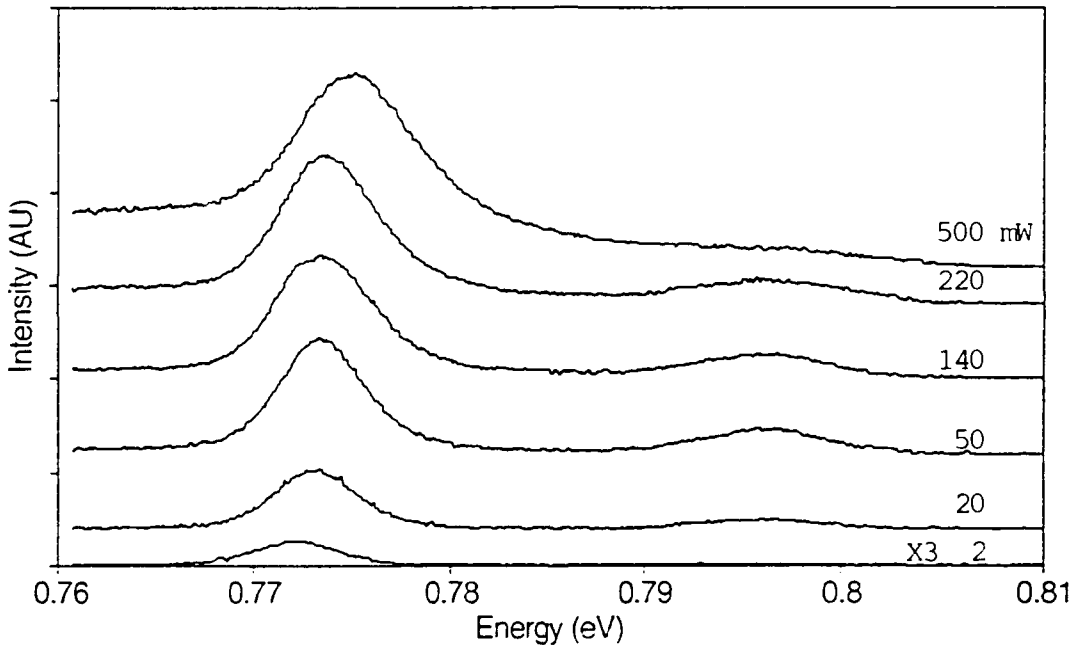

Figure 15. Excitation Power Dependence Spectra of Intermediate Antimony Flux GaSb

emission was not observed in the spectra, six of which are shown in Figure 15. The integrated intensity of the emission increased with laser power and no saturation of the transition was observed up to 500 mW. Figure 16 shows the change in energy and intensity of the peak associated with the native acceptor emission.

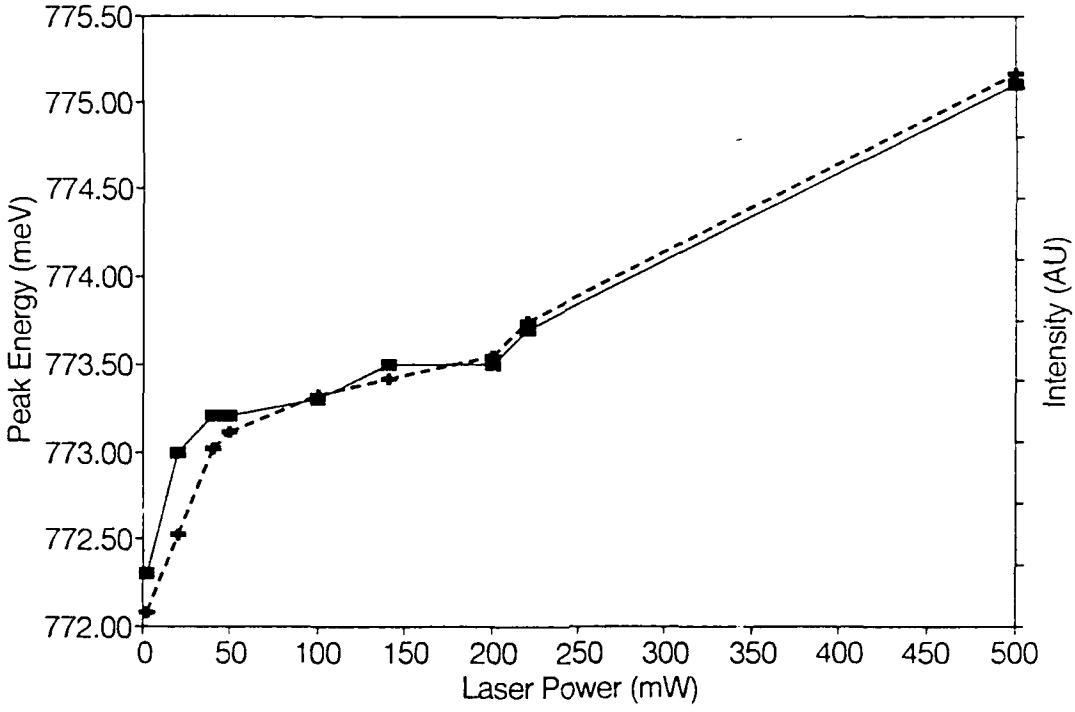

Figure 16. Excitation Power Dependence of Native Acceptor Peak Energy (solid) and Intensity (dash) for Sample 90-088

The attempt to investigate the power dependence of sample 90-097 was not successful. Though numerous alignments were attempted, the signal remained weak at all powers, see Figure 17. The noise in the signal is evident because a high sensitivity was required to observe the signal. This difficulty may be due to quality and/or the inhomogeneity of the sample.

On the other hand, the temperature dependence study was very fruitful. This sample was grown in a higher antimony flux environment than sample 90-088. This resulted in a significantly different spectra, in fact the broad emission is similar to the previously discussed n-type GaSb. The laser was operated at 100 mW for this study and the temperature ranged from 4 to 150 K in 10 steps. Three peaks were noted for the spectra, 771.9, 760.2, and 751.3 meV, see Figure 18, which shows

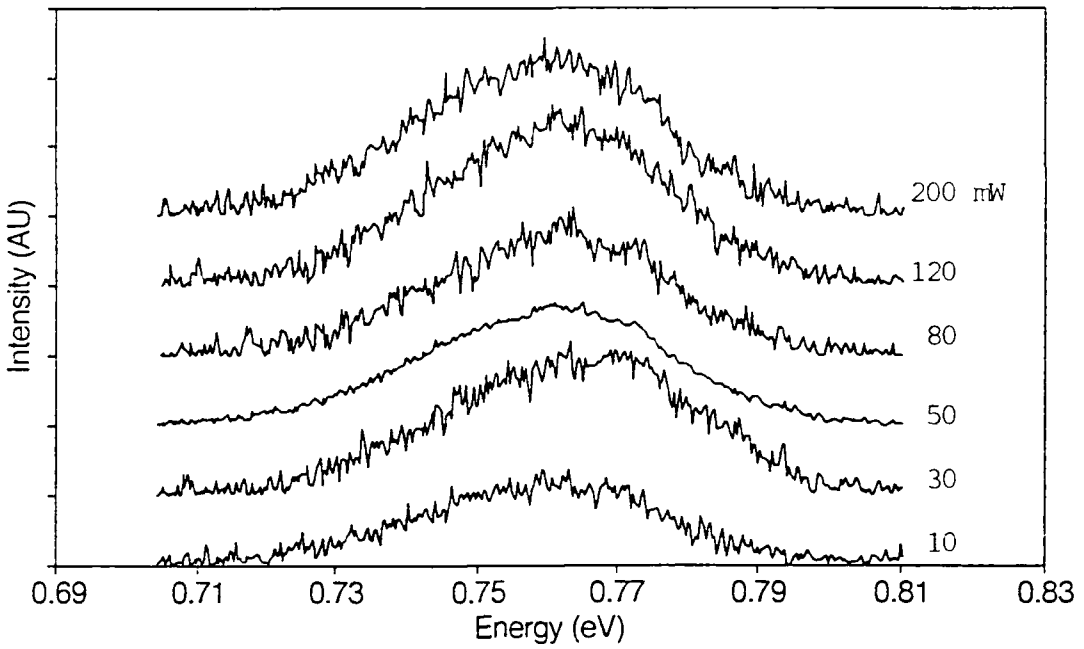

Figure 17. Excitation Power Dependence Spectra of High Antimony Flux GaSb for Sample 90-097

six spectra. The energy of the peaks does not appear to shift with temperature. The apparent but slight changes in the 760 meV peak are attributed to the noise in the data. The rapid decrease in the 772 meV emission with increased temperature is indicative of a donor-acceptor pair transition. The ionization of the donor levels occurs rapidly with temperature; this line may be related to the native acceptor. In comparing the relative intensity of the other two emissions, the 751 meV peak resists suppressing with temperature in comparison to the 760 meV peak. The persistence of both of these peaks with temperature strongly suggests they are due to a free-to-bound transition. The high antimony flux during growth should have increased the antimony antisite defects. In addition to a deep acceptor complex, a deep level donor complex can be a possible explanation for the peak with the persistence due to the depth of the complex.

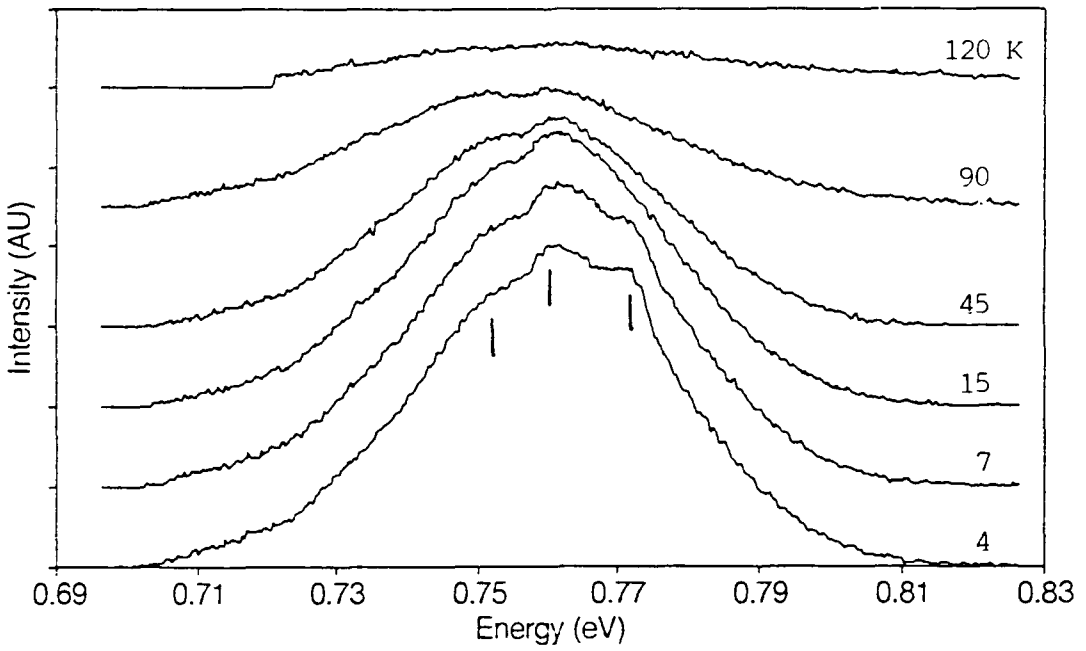

Figure 18. Temperature Dependence Spectra of High Antimony Flux GaSb of Sample 90-097

During an attempt to measure the photoluminescence of sample 90-098 a phenomena was observed that had earlier been observed on sample 90-250 with cathodoluminescence. The intensity of an emission peak varied with time with the application of the laser or electron beam. After the initial exposure of the sample the beam was blocked. Upon unblocking the source, the intensity would rise to a maximum in 2 to 4 seconds, followed by a decline lasting an additional 1 to 2 seconds. The final intensity level was the same as the intensity prior to blocking the source. With cathodoluminescence the variation was ascribed to heating of the sample, which did increase some emissions. However the heating effect was not a likely cause with the photoluminescence. The observed effect is similar to the photoluminescence fatigue and recovery effect discussed by Tajima for

deep levels in GaAs (25:52). He associates the recovery effect with "the existence of the metastable states with large lattice relaxation" (25:53).

The cathodoluminescence of GaSb was measured for a sample not measured in this photoluminescence study. A weak signal intensity and competing and occasionally dominant signal from the filament generating the electrons made measurement difficult. The results were not conclusive, but a single spectrum showed a broad luminescence emission with a center energy of about 750 meV and a FWHM of about 45 meV, see Figure 19. An explanation of the emission might be due to experimental methods, the use of a copper based vacuum grease to mount the sample, or to unanticipated emission from the n-type GaSb substrate.

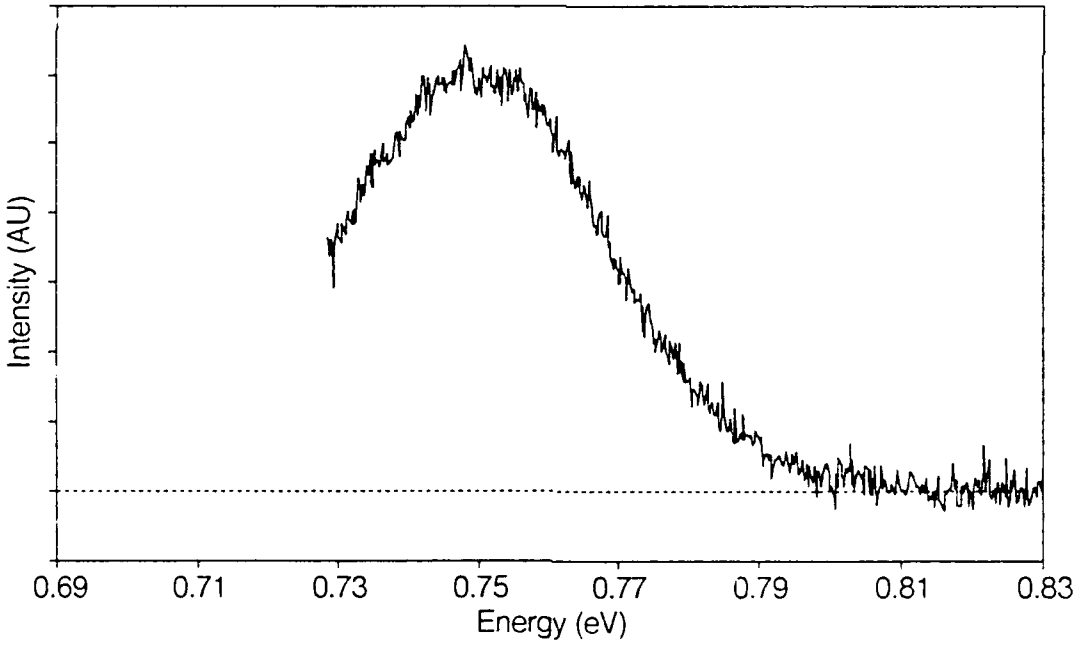

Figure 19. Cathodoluminescence Spectrum of Undoped GaSb

The cathodoluminescence from a well investigated sample of $Al_{.5}Ga_{.5}As$ doped with erbium (26) was measured to judge the operation of the cathodoluminescence set-up. The erbium related transitions occur near 1.54 μm. When examined, with the same photoluminescence set-up as used for the GaSb samples, the spectra in Figure 20 was obtained. For cathodoluminescence the sample was investigated at a beam current of 20 mA and beam energies from 2100 to 4200 V, with resulting beam powers of 42 to 84 mW. The results, in Figure 21, show a strong similarity to the photoluminescence spectra. This comparison gives a confidence that the method of cathodoluminescence hold the possibility of further results in the investigation GaSb and GaAsInSb.

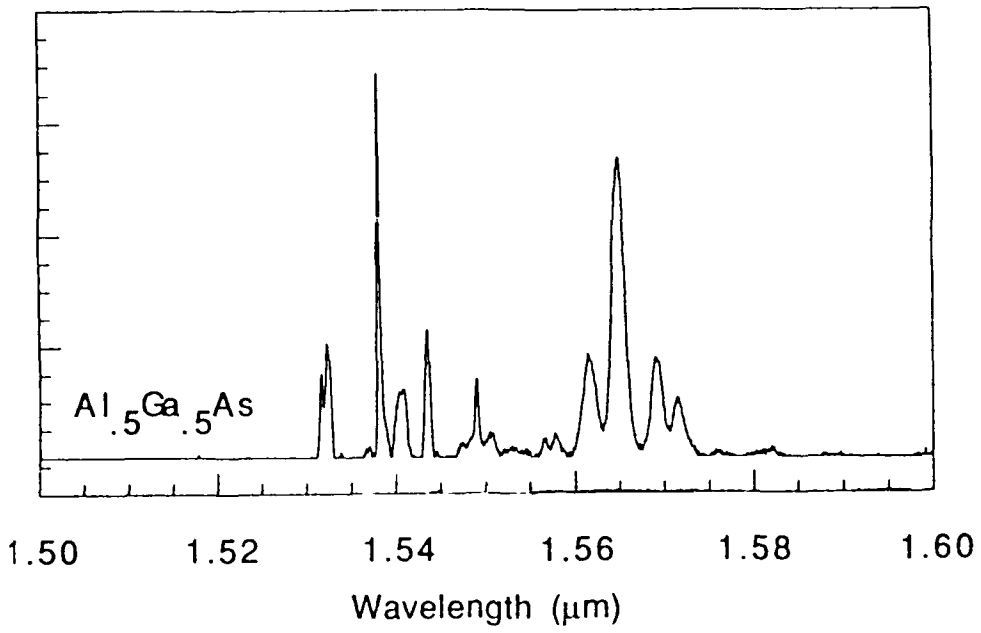

Figure 20. Spectrum of $Al_{.5}Ga_{.5}As$:Er from Photoluminescence

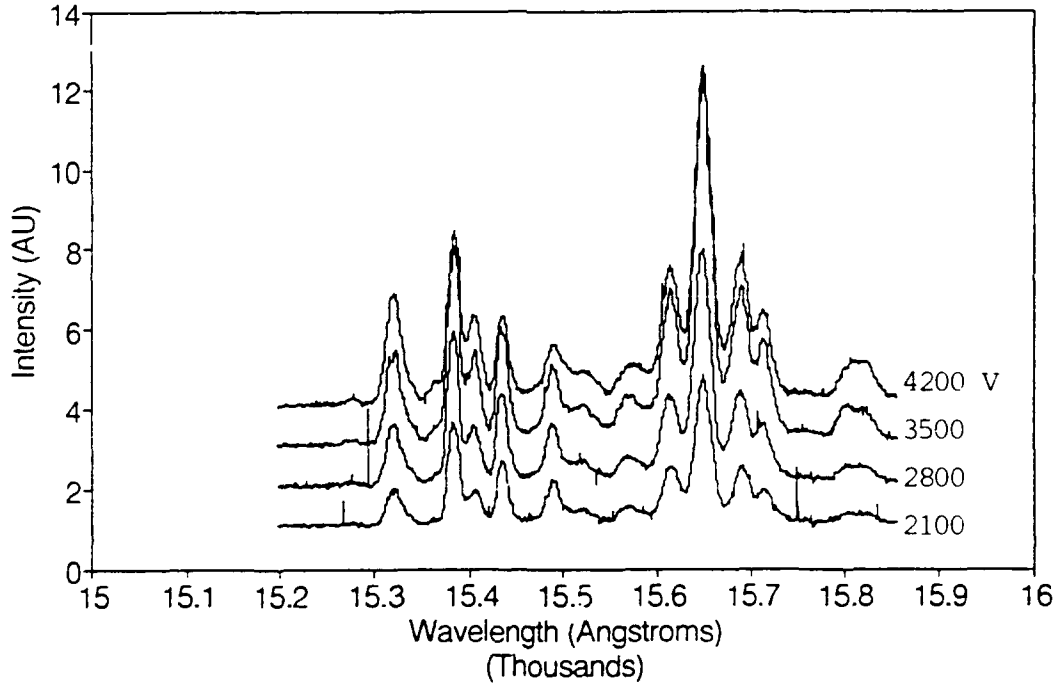

Figure 21. Spectrum of $Al_{.5}Ga_{.5}As$:Er from Cathodoluminescence

V. Conclusion and Recommendations

The direct transition semiconductor gallium antimonide has been studied by photoluminescence spectroscopy. The investigations of this material stretch back over thirty years and yield a number of reports about the material and its luminescence, although molecular beam expitaxial grown GaSb is a relatively recent addition to the list of topics. The low temperature photoluminescence experimental set-up involved an argon ion laser and a germanium detector.

The emission from undoped p-type GaSb was observed and matched well with the luminescence from GaSb grown by other methods. The dominant emission, at 776 meV, was noted to be associated with a donor acceptor transition, with the acceptor complex (V_{Ga}-Ga_{Sb}) having a neutral energy level at 35 meV above the valence band, and the first ionized level at 95 meV. In one sample the bound exciton emissions were quite pronounced. In GaSb grown with a high antimony flux the emission structure changed to a broad luminescence due to three different transitions. At 772 meV was a donor-acceptor transition that disappeared with increasing temperature, while peaks at 760 and 751 meV, associated with either acceptor free-to-bound or a deep donor level, persisted at the elevated temperatures. The luminescence from a tellurium doped n-type GaSb was observed to be broad, a result correlated with the high electron concentration. The effect of a lattice mismatch was observed in the n-type samples as a reduction in the intensity of the emission. The technique of cathodoluminescence was

briefly studied to assess the possibility of future examination of GaSb and GaAsInSb.

Further photoluminescence studies should be performed to assess the extent of the homogeneity of the samples, since reproducibility of the data is dependent on this knowledge. Also a further study could profitably investigate the tellurium doped GaSb, to include temperature and power dependence, to assess the sources of the emissions. Finally, an assurance of replicable data can be enhanced by a separate investigation of the intensity variation of sample 90-098, seeking to determine if temperature dependence or a fatigue and recovery effect is the basis of the variation. The use of time resolved measurements would be appropriate and informative.

The experimental approach would greatly benefit from an electron gun which is reliable and permits modulation of the beam, for use with a lock-in amplifier. The data reduction effort may be enhanced with improved personal computer based software for data averaging to reduce noise and for the identification of emission energies when multiple peaks overlap. Also, other spectroscopic techniques for low intensity emissions should be investigated.

Consideration of cathodoluminescence spectroscopy for examination of the GaSb and GaAsInSb samples should be encouraged. The broad energy distribution of the electrons and a suitably sensitive detector operating at longer wavelengths, greater than 1.75 μm, are attainable elements which will permit fuller studies of photosensitive materials that may have a role to play in future Air Force communication, guidance and detection systems.

Appendix 1

The penetration of the laser into the semiconductor is determined by the extinction coefficient of the material and the wavelength of the incident photon. The extinction coefficient is shown below for a temperature of 300 K (27:525). For the 488 nm argon laser the equation for absorption coefficient, in inverse centimeters, is:

$$\alpha = 4\pi K/(.488 \times 10^{-4}) \quad (7)$$

And for a penetration depth of 1/e (37%), the depth satisfies:

$$\exp(-\alpha x) = 1/e \quad (8)$$

Table 9. Argon Laser Penetration into Gallium Antimonide at 300 K

Wavelength (μm)	K	α (cm^{-1})	Depth (μm)
1.51	0.0945	24334.5	0.411
1.53	0.0916	23330.2	0.429
1.57	0.0816	21012.6	0.476
1.59	0.0768	19776.6	0.506
1.61	0.071	18283.0	0.547
1.63	0.0649	16712.2	0.598
1.65	0.0582	14986.9	0.667
1.66	0.0547	14085.7	0.71
1.69	0.047	12102.9	0.826
1.71	0.0251	6463.4	1.547
1.73	0.0067	1720.2	5.813

Appendix 2

The choice of units for expressing laser power on the sample is not definitive. The use of a power density is better but entails some knowledge of the losses of the beam power at the windows of the dewar. The spot size for the laser is estimated to be 3 mm in diameter, for an area of 0.0707 cm^2. This area leads to an approximate power density of the following values.

Table 10. Laser Power Density

Beam Power (mW)	Power Density (W/cm^2)
2	.028
20	.283
40	.566
50	.707
70	.990
100	1.414
140	1.980
200	2.829
220	3.112
500	7.072

Appendix 3

The Spex 1702 spectrometer was operated at different slit widths during scans of the same sample. By comparing intensities of scans that were identical except for the slit width the following adjustment factors were determined. The entrance and exit slits were set to the same spacing during the recording of the data.

Table 11. Spectrometer Slit Adjustments

Setting 1	Setting 2	Factor
1000/1000	500/500	3.776
800/800	400/400	3.624
400/400	200/200	4.827

Appendix 4

During a significant portion of the thesis research, the focus was on the cathodoluminescence spectroscopy. A description of the equipment collected for those measurements follow. See Figure 22.

The luminescence of the samples was measured in a 0.05 m^3 vacuum chamber which could attain a vacuum of 10^{-9} torr. The sample was cooled using a liquid helium transfer line and cold-finger, and regulated with a temperature controller which employs resistive heaters. The excitation mechanism was predominantly with an electron gun, however a laser was occasionally used for comparison. The luminescent signal was collected with lenses into a spectrometer and detector. During different phases of the experiment either a lead sulfide (PbS) or germanium (Ge) detector was used. The signal from the detector was amplified and then recorded and stored on a computer diskette.

The vacuum system was a cylindrical chamber, 0.67 meter high by 0.3 meter in diameter, with three different oil-free pump units. Two Varian VacSorb cryo-sorbtion pumps were attached through manifolds, which were valved to also allow the pressure of the chamber to be raised to atmospheric pressure. One Varian Titanium Sublimation Pump, Model 916-0017, and control unit, Model 922-0052 was mounted in the bottom half of the chamber. A Varian 110 liter/second Noble VacIon Pump, Model 921-0041, and control unit, Model 916-0043, was also mounted in the bottom half. The VacIon pump was operated as the only pump once pressures below 1 x 10^{-7} torr were achieved. The pressure in the chamber was measured with a Granville-Phillips ionization gauge, or the current versus pressure curve of the VacIon pump. In the top half of

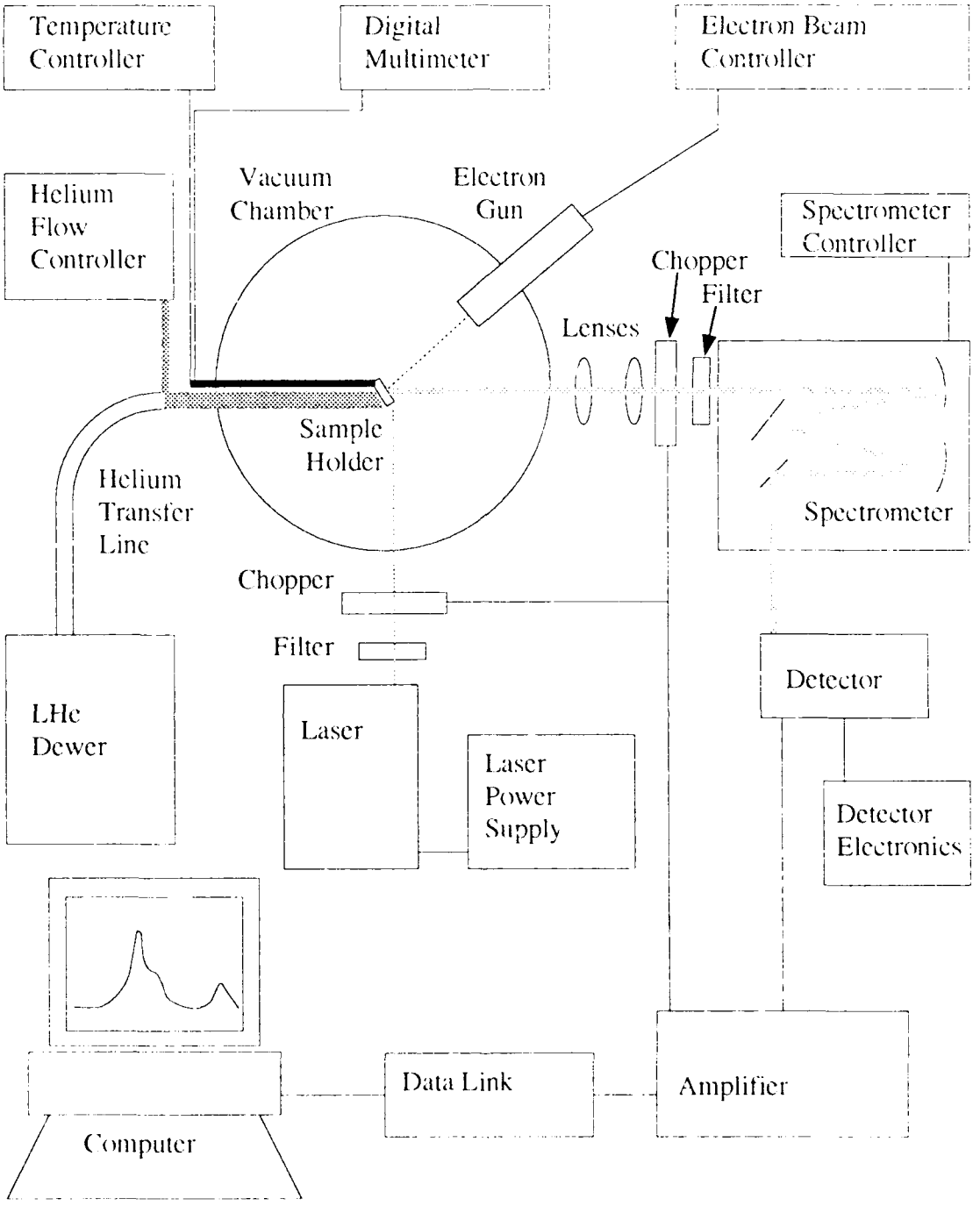

Figure 22. Cathodoluminescence Experiment Laboratory

the chamber were mounted two optical windows. One was a glass window held at the Brewster angle; it was through this window that the laser entered the chamber. The second window was an exit port for the sample luminescence. It was two inches in diameter and made of sapphire.

An Air Products Heli-Tran system, Model LT-3-110, transferred liquid helium from a standard dewar to the cold-finger. The transfer line used two capillary sized tubes to flow the liquid helium and provide heat exchange. The exhaust gases of the cold-finger and the transfer line were regulated at a control panel to moderate the temperature of the sample. The end of the Heli-Tran which attached to the vacuum chamber could be rotated easily, allowing the sample to face either the laser or the electron beam. Due to the high vacuum environment, the samples were held in place with Air Products Cry-Con grease. The grease held the sample securely in place and offered adequate heat transfer properties. The grease was spread in a band across the sample, covering about 25 percent of the back surface. The Heli-Tran refrigerator, or cold-finger, attached to the transfer line and held the Cryo-Tip which is a copper block holding the sample, resistive heaters, and temperature sensors. A gold-chromel thermocouple was connected to a Systron Donner digital multi-meter, Model 7000A, to measure a millivolt scale reading that was reference to a temperature. In addition, a Lake Shore Cryotronics temperature controller, Model DRC 80C, measured temperature and operated the resistive heaters. The temperature controller applied current to the heaters when it sensed a difference between a preset and the measured temperature. Temperature control was accurate to 0.1 K, with a lower temperature bound of 8 K achieved during the experiment.

The primary excitation mechanism for this experiment was cathode rays, also known as an electron beam. A VG Industries Leg 32 electron gun was the source, and it was used in conjunction with a Model 326A power supply. The gun permits beam energies of 0.1 to 5 keV, and beam currents of 2 to 1000 μA. The beam is electrostatically focused and can be steered by a quadrupole arranged element. The power supply allows a dial-in selection of the beam energy in 100 eV steps while a continuous dial is used to set the filament current. The resulting beam current is displayed on a gauge mounted in the power supply.

A Spectra-Physics Argon Ion laser, Model 161B-07 with a modified Model 262A power supply, was available to perform low power photoluminescence experiments. This laser produced 488 nm wavelength light with a measured power of 25 mW. An Oriel band pass filter, Model 52640, with a center wavelength of 488 nm, was used to eliminate unwanted laser emissions. During photoluminescence measurements an EG&G Princeton Applied Research Variable Frequency Light Chopper, Model 192, was placed after the filter and before the window.

The emissions from the excited sample were collected and detected to create a signal which could be accurately and rapidly recorded. The emission, after passing through the vacuum chamber window, was collected and focused by a lens system. The lenses focused the emission through a 1 μm long pass filter onto the entrance slit of the spectrometer. During cathodoluminescence measurements the light chopper was place between the lenses and the long pass filter.

A Spex 500M Spectrometer and an MSD 2 controller were used to separate the emitted luminescence into the different wavelengths. The

controller allowed the selection of a continuous range of scan rates, though a metered dial on the controller permitted the scan rate to be duplicated when required. The scan rate was typically 100 Angstroms/minute. Two gratings were used to compliment the detector selected at the time. When the Ge detector was used, a Milton Roy 600 lines/mm 1.6 μm blazed grating was installed. For the PbS detector, a Milton Roy 300 lines/mm 3.0 μm blazed grating was used.

A North Coast Scientific Corporation germanium detector, Model EO-817S, was initially used to judge system performance and attain data on the GaSb samples. This detector covered a range from 800 to 1700 nm. It was kept at liquid nitrogen temperatures during operation and a bias voltage of -250 V was provided by a North Coast Scientific Bias Supply, Model 823A. No muon filter was used on the recommendation of the manufacturer. The signal from the Ge detector was fed directly into the amplifier, as described below.

A New England Photoconductor lead sulfide detector, Series EM, S/N 24024, was used to cover the wavelength range from 1 to 3.5 μm; it allowed observation of the GaAsInSb emissions. The detector was cooled with liquid nitrogen and was biased with a laboratory built circuit. The time constant of the detector was 4300 μsec and the specific detectivity (D*) was 2.15×10^{11} cm$(Hz^{\frac{1}{2}})$/W. Coaxial cable was used to reduce the noise on the signal. A dry cell battery supplying 180 V into a 5.65 MΩ resistor provided a small current through the detector. The signal out of the detector was capacitively coupled through a 0.001 μF capacitor to the amplifier. The capacitor prevented the high DC bias

voltage from reaching the amplifier, while still allowing the AC signal to be accepted.

Either detector was then connected to a Keithley 840 Autoloc Amplifier. The amplifier had an input from the chopper as a reference and a second input from the detector. The amplifier compared the signal when the luminescence was present to when it was only background with phase sensitive detection to only permit the desired signal to be measured. Typical settings for GaSb measurements were a time constant of 300 msec and a sensitivity of 0.3 mV. The output of the amplifier was sent to a MetraByte STA-16 DAS-16 Accessory board which was matched to a MetraByte DASH-16 internal data acquisition board in a Zenith Data Systems Z248 computer. The software used to monitor the data collection was Labtech Notebook. Typically, data was collected at a rate of 5 Hz for a duration of 20 minutes. The data was recorded on diskette in ASCII format and was available for manipulation and plotting by many routines, including the spreadsheet Quattro Pro.

Bibliography

1. Eglash, S. J. and others. "MBE Growth of GaAsInSb/AlGaAsSb Double Heterostructures for Infrared Diode Lasers," Journal of Crystal Growth, 111: 669-676, (May 1991).

2. Tournié, E. and others. "2.5 μm GaAsInSb Lattice-Matched to GaSb by Liquid Phase Epitaxy," Journal of Applied Physics, 68: 5936-5938 (1 December 1990).

3. Pankove, Jacques I. Optical Processes in Semiconductors. Englewood Cliffs, NJ: Prentice-Hall, 1971.

4. Dekeyser, W.C. "Crystal Structure," Solid State Physics Source Book edited by Sybil Parker. New York: Magraw-Hill, 1988.

5. Woelk, C. and K. W. Benz. "Gallium Antimonide LPE Growth from Ga-Rich and Sb-Rich Solutions," Journal of Crystal Growth, 27: 177-182, (1974).

6. Rühle, W. and D. Bimberg. "Linear and Quadratic Zeeman Effect of Excitons Bound to Neutral Acceptors in GaSb," Physical Review B, 12: 2382-2390 (15 September 1975).

7. Lee, M. and others. "A Photoluminescence and Hall-Effect Study of GaSb grown by Molecular-Beam Epitaxy," Journal of Applied Physics, 59: 2895-2900 (15 April 1986).

8. Moses, Alfred J. The Practicing Scientist's Handbook. New York: Van Nostrand Reinhold, 1978.

9. Hilsum, C. "Some Key Features of III-V Compounds," Semiconductors and Semimetals, Volume 1, edited by R. K. Willardson and A.C. Beer. New York: Academic Press, 1966.

10. Long, Donald. "Band Structures of Mixed Crystals," Semiconductors and Semimetals, Volume 1, edited by R. K. Willardson and A.C. Beer. New York: Academic Press, 1966.

11. Gershenzon, M. "Radiative Recombination in the III-V Compounds," Semiconductors and Semimetals, Volume 2, edited by R. K. Willardson and A.C. Beer. New York: Academic Press, 1966.

12. Su, Y. K. and others. "Raman Spectra of Si-Implanted GaSb," Journal of Applied Physics, 68: 5584-5587 (1 December 1990).

13. Nakashima, Kenshiro. "Electrical and Optical Studies in Gallium Antimonide," Japanese Journal of Applied Physics, 20: 1085-1094 (June 1981).

14. Chen, S. C. and Y. K. Su, "Photoluminescence Study of Gallium Antimonide Grown by Liquid-Phase Epitaxy," Journal of Applied Physics, 66: 350-353 (1 July 1989).

15. Bochkarev, A. É. and others. "Photoluminescence of Epitaxial GaSb Films and of GaAsInSb Solid Solutions," Soviet Physics: Semiconductors, 16: 1215-1216 (October 1982).

16. Zimogorova, N. S. and others. "Photoluminescence Parameters of Epitaxial P-Type Gallium Antimonide Films," Soviet Physics: Semiconductors, 17: 1427-1428 (December 1983).

17. Baranov, A. N. and others. "Photoluminescence of Epitaxial Gallium Antimonide Films Grown from Antimony-Rich Melts," Soviet Physics: Semiconductors, 19: 1030-1032 (September 1985).

18. Poole, I. and others. "Deep Donors in GaSb Grown by Molecular Beam Epitaxy," Applied Physics Letters, 57: 1645-1647 (15 October 1990).

19. Haywood, S. K. and others. "GaSb/GaInSb Quantum Wells Grown by Metalorganic Vapor Beam Epitaxy," Applied Physics Letters, 54: 992-995 (6 March 1989).

20. Eglash, S. J. and others. "MBE Growth of GaAsInSb/AlGaAsSb Double Heterostructures for Diode Lasers Emitting beyond 2 μm," Material Research Society Symposium Proceedings, 216, (1991).

21. Davies, G. J. and D. Williams. "III-V MBE Growth Systems," The Technology and Physics of Molecular Beam Epitaxy, edited by E. H. C. Parker. New York: Plenum Press, 1985.

22. Eglash, Stephen J., Technical Staff Member. Personal Correspondence. Massachusetts Institute of Technology, Lincoln Laboratory, Lexington, MA, 25 June 1991.

23. Dean, P. J. "Photoluminescence as a Diagnostic of Semiconductors," Progress in Crystal Growth Characterization, 5: 89-174 (1982).

24. Nicholas, D. J. and others, "Spectroscopic Studies of Shallow Defects in MBE GaSb," Journal of Crystal Growth, 81: 298-303, (1987).

25. Tajima, Michio. "Deep Level Photoluminescence in GaAs," Defects and Properties of Semiconductors: Defect Engineering. Tokyo: KTK Scientific Publishers, 1987.

26. Evans, K. R. and others. "Molecular Beam Epitaxial Growth and Characterization of Erbium-Doped GaAs and AlGaAs," Proceedings of the 11th MBE Workshop. Austin, TX, 1991. To be published in the Journal of Vacuum Science.

27. Seraphin, B. O. and H. E. Bennett. "Optical Constants," Semiconductors and Semimetals, Volume 3, edited by R. K. Willardson and A.C. Beer. New York: Academic Press, 1967.